Notes on the Hartee-Fock method and its applications

W. Zhu[1]

[1] *Westlake Institute of Advanced Study,*

Westlake University, Hangzhou, P. C. China

Contents

Self-consistent Hartee-Fock Approximation 2

Application: Interacting fermions 4

Application: Density Functional Theory 9

Application: Topological Mott Insulator on the honeycomb lattice 13

Application: The Hubbard model 18

Conduction limit $U \to 0$ 20

Atomic limit $U \to \infty$ 22

Interaction terms U 23

Computational details. 24

Discussion of results: phase diagram. 28

Generalizations and conclusion. 30

Application: Twisted Graphene/TMD systems 33

Homework 38

References 38

Many electronic properties of condensed matter systems can be understood using an independent-electron approximation, in which each electron moves in an identical external potential. In this chapter we will first discuss how this reduction from a many-body problem to a single-particle problem is carried out systematically for the ground state, using a traditional mean-field method. It can be in principle generalized to study response functions and (certain) collective excitations of the system.

The Hartree-Fock method is a basic method for approximating the solution of many-body electron problems in atoms, molecules, solids, and nuclear physics, and in other applications. In the Hartree-Fock method, one attempts to find the best multi-particle state that can be represented as a Slater determinant of single particle states, where the criterion for "best" is the usual one in the variational method in quantum mechanics. For the Hartree-Fock method, this means that the expectation value of the energy should be stationary with respect to variations in the single particle orbitals. Hartree-Fock solutions are often used as a starting point for a perturbation analysis, which is capable of giving more accurate approximations.

SELF-CONSISTENT HARTEE-FOCK APPROXIMATION

The physics of interacting particles is often very complicated because the motions of the individual particles depend on the position of all the others, or in other words the particles motions become correlated. This is clearly the case for a system of charged particles interacting by Coulomb forces, such as e.g. the electron gas, as shown above. Nevertheless, in spite of this complicated problem there are a number of cases where a more crude treatment, not fully including the correlations, gives a good physical model. In these cases it suffices to include correlations "on the average", which means that the effect of the other particles is included as a mean density (or mean field), leaving an effective single particle problem, which is soluble. The mean fields are chosen as those which minimize the free energy, which in turn ensure that the method is consistent, as we shall see shortly. This approximation scheme is called "mean-field theory".

In general, the hmailtonian will be like $H = H_0 + V_{int}$. The interaction V_{int} is approximated by the mean field interaction V_{MF} resulting in the so-called mean field Hamiltonian H_{MF} given by $H_{MF} = H_0 + V_{MF}$. The mean field Hamiltonian H_{MF} contains only

single-particle operators, and thus the original many-body problem has been reduced to a single-particle problem, which in principle is always soluble.

Say, we have a system as

$$H = H_A + H_B + H_{AB} = f(A) + g(B) + \lambda AB \tag{1}$$

where AB is the interaction between A and B. The simplest treatment is

$$AB \approx A\langle B\rangle + \langle A\rangle B - \langle A\rangle\langle B\rangle. \tag{2}$$

$\langle A\rangle$ is the averaged value of operator A over the mean-field ground state. It is a c-number. To get a proper value of $\langle A\rangle$ is the the central target of the mean-field calculation. There are two possible routes to get solution which in fact are equivalent.

Method 1 The average is to be determined self-consistently, i.e. when calculating the averages $\langle A\rangle = \frac{1}{Z_{MF}} Tr[e^{-\beta H_{MF}} A]$, and same with $\langle B\rangle$, where $Z_{MF} = Tr[e^{-\beta H_{MF}}]$ is the mean field partition function. This is a self-consistency equations.

Method 2 Using the $\langle A\rangle, \langle B\rangle$ to minimize the free energy F_{MF} of the mean field Hamiltonian. Using the expression for the free energy $F_{MF} = -\ln Z_{MF}$ givenv $\frac{\partial F_{MF}}{\partial \langle A\rangle} = 0, \frac{\partial F_{MF}}{\partial \langle B\rangle} = 0$. One can see that the two methods are equivalent.

Last but not least, the choice of the proper mean field parameters requires physical motivation about which possible states one expects. You will see many examples next.

Using the two-body electron-electron interaction as example, we present how it works in practice.

$$V_{int} = \sum_{a,b,a',b'} V_{ab,a'b'} c_a^+ c_b^+ c_{b'} c_{a'} \tag{3}$$

The basic idea behind the mean field theory was that the operator $n_{aa'} = c_a^+ c_{a'}$ is large only when the average $\langle n_{aa'}\rangle$ is non-zero. For most of the combinations the average $\langle n_{bb'}\rangle$ is zero. We therefore use the same strategy and write the four operators in the interaction term in terms of a deviation from the average value

$$c_b^+ c_{b'} \langle c_a^+ c_{a'}\rangle + c_a^+ c_{a'} \langle c_b^+ c_{b'}\rangle - \langle c_b^+ c_{b'}\rangle \langle c_a^+ c_{a'}\rangle \tag{4}$$

Thus we arrived at the Hartee approximation for interactions

$$V_{int}^{Hartee} = \sum V_{ab,a'b'} n_{aa'} c_b^+ c_{b'} + \sum V_{ab,a'b'} n_{bb'} c_a^+ c_{a'} - \sum V_{ab,a'b'} n_{aa'} n_{bb'} \tag{5}$$

This is not the full result. To derive the mean field contribution from another possibility we thus have to first replace $c_a^+ c_{b'}$ by its average value and following the mean-field principle

$$V_{int}^{Fock} = -\sum V_{ab,a'b'} n_{ab'} c_b^+ c_{a'} - \sum V_{ab,a'b'} n_{ba'} c_a^+ c_{b'} + \sum V_{ab,a'b'} n_{ab'} n_{ba'} \tag{6}$$

Again we emphasize that the Hartree–Fock approximation depends crucially on what averages we assume to be finite, and these assumptions must be based on physical knowledge or clever guess-work (see examples below).

APPLICATION: INTERACTING FERMIONS

We consider the weakly interacting fermions in solids, where the electrons are interacting with each other via long-ranged Coulomb interaction as a starting point. The hamiltonian describes N electrons moving in a uniform ion background:

$$H = H_{elec} + H_{background} + H_{elec-background} \tag{7}$$

$$H_{elec} = \sum_{j=1}^{N} \frac{p_j^2}{2m} + \frac{1}{2} \sum_{i \neq j} \frac{(-e)^2}{|r_i - r_j|} \tag{8}$$

$$H_{background} = \frac{1}{2} e^2 \int d^3x \int d^3x' \frac{n_b(x) n_b(x')}{|x - x'|} \tag{9}$$

$$H_{elec-background} = -e^2 \sum_{j=1}^{N} \int d^3x \frac{n_b(x')}{|x - r_j|} \tag{10}$$

where $H_{background}$ is the uniform positive change background, $H_{elec-background}$ is interaction between electron and background charges energy. To separate the symbols, we use r_i to represent electron coordinates and x_i the ion coordinates. Please note that, we neglect the kinetic energy of $H_{background}$, since we approximate ion is heavy enough. This is called Born-Oppenheimer approximation (discussed below). To keep the the whole system charge neutral, we assume number of ions is equal to number of electrons (each ion takes the charge $+e$). Then we define the density is almost uniformed distributed and $n_b = N/V$ is a constant.

For the electron Hamiltonian, we write it using second quantization:

$$H_{elec} = \sum_{\mathbf{k}} \epsilon^0(\mathbf{k}) c_{\mathbf{k}}^\dagger c_{\mathbf{k}} + \frac{1}{2} \sum_{\mathbf{k}_1, \mathbf{k}_2, \mathbf{q}} V(\mathbf{q}) c_{\mathbf{k}_1 + \mathbf{q}}^\dagger c_{\mathbf{k}_2 - \mathbf{q}}^\dagger c_{\mathbf{k}_2} c_{\mathbf{k}_1} \tag{11}$$

where the kinetic energy is $E^0(\mathbf{k}) = k^2/2m$. The interaction term is

$$V(\mathbf{q}) = \frac{1}{V^2}\int d\mathbf{x}d\mathbf{x}' e^{-i(\mathbf{k}_1+\mathbf{q})\mathbf{x}} e^{-i(\mathbf{k}_2-\mathbf{q})\mathbf{x}'} \frac{(-e)^2}{\epsilon|\mathbf{x}-\mathbf{x}'|} e^{i\mathbf{k}_1\mathbf{x}} e^{i\mathbf{k}_2\mathbf{x}'} = \frac{1}{V^2}\int d\mathbf{x}d\mathbf{x}' e^{i\mathbf{q}(\mathbf{x}-\mathbf{x}')} \frac{(-e)^2}{\epsilon|\mathbf{x}-\mathbf{x}'|}$$
$$\Rightarrow V(\mathbf{q}=0) = \frac{1}{V^2}\int d\mathbf{x}d\mathbf{x}' \frac{(-e)^2}{\epsilon|\mathbf{x}-\mathbf{x}'|} = \frac{1}{V}\int d\mathbf{z}\frac{(-e)^2}{\epsilon|\mathbf{z}|} \tag{12}$$

Then we estimate the contribution of term $V(0)$ in electron-electron interaction

$$\begin{aligned}\langle 0|H_{ee,q=0}|0\rangle &= \frac{1}{2}V(0)\sum_{\mathbf{k}_1,\mathbf{k}_2}\langle 0|c^\dagger_{\mathbf{k}_1}c^\dagger_{\mathbf{k}_2}c_{\mathbf{k}_2}c_{\mathbf{k}_1}|0\rangle \\ &= \frac{1}{2}V(0)\sum_{\mathbf{k}_1,\mathbf{k}_2}\langle 0|c^\dagger_{\mathbf{k}_1}c_{\mathbf{k}_1}c^\dagger_{\mathbf{k}_2}c_{\mathbf{k}_2}|0\rangle - \frac{1}{2}V(0)\sum_{\mathbf{k}_1}\langle 0|c^\dagger_{\mathbf{k}_1}c_{\mathbf{k}_1}|0\rangle \\ &= \frac{1}{2}V(0)(N^2-N) \approx \frac{1}{2}\frac{N^2}{V}\int d\mathbf{z}\frac{(-e)^2}{\epsilon|\mathbf{z}|}\end{aligned} \tag{13}$$

Similarly, we can estimate the energy of background term as

$$H_{background} = \frac{1}{2}\int d\mathbf{x}d\mathbf{x}'\frac{(+e)n_b(x)(+e)n_b(x')}{\epsilon|x-x'|} \approx \frac{1}{2}\frac{N^2}{V^2}\int d\mathbf{x}d\mathbf{x}'\frac{e^2}{\epsilon|\mathbf{x}-\mathbf{x}'|} = \frac{1}{2}\frac{N^2}{V}\int d\mathbf{z}\frac{e^2}{\epsilon|\mathbf{z}|} \tag{14}$$

and electron-background part is

$$H_{elec-background} = \sum_{j=1}^{N}\int d\mathbf{x}\frac{(+e)n_b(x)(-e)}{|x-r_j|} = -\frac{N^2}{V}\int d\mathbf{z}\frac{e^2}{\epsilon|z|} \tag{15}$$

To sum up, we see that $H_{background} + H_{ee,q=0} + H_{elec-background} = 0$, because $H_{elec-background}$ takes the opposite sign and twice of $H_{background}, H_{ee,q=0}$. This remarkable result means, even though $V(0)$ itself is divergent, we can safely remove $q = 0$ term in the Hamiltonian. Below we will discuss the final hamiltonian as our target:

$$H = \sum_{\mathbf{k}} E^0(\mathbf{k})c^\dagger_{\mathbf{k}}c_{\mathbf{k}} + \frac{1}{2}\sum_{\mathbf{k}_1,\mathbf{k}_2,\mathbf{q}\neq 0} V(\mathbf{q})c^\dagger_{\mathbf{k}_1+\mathbf{q}}c^\dagger_{\mathbf{k}_2-\mathbf{q}}c_{\mathbf{k}_2}c_{\mathbf{k}_1} \tag{16}$$

To reach the above model hamiltonian, we have used the Born-Oppenheimer approximation: the electrons quickly adjust their state to reflect whatever positions the ions occupy at any given time, i.e. to a good approximation, one may solve the Schrodinger equation for electrons by assuming that the ions are fixed. Moreover, that the divergent term in the Coulomb interaction corresponding to $q = 0$ (see above) is canceled by contributions to the total energy from the positive background, makes the so-called the jellium model. This cancellation is a consequence of the charge neutrality of the crystal.

Under what conditions could the Coulomb interaction between electrons be treated as a small perturbation? To answer this question, we need introduce a parameter. If the averaged distance between electrons is r_0, since $\frac{4\pi}{3}r_0^3 N = V$, we have $r_0 = (4\pi/3)^{-1/3}(N/V)^{-1/3} \sim n^{-1/3}$. So high density leads to small distance $r_0 \ll 1$. And $n = k_F^3/(3\pi^2)$ ($N = \frac{\frac{4\pi}{3}k_F^3}{(2\pi/L)^3} \times 2$), we have $r_0 = (9\pi/4)^{1/3}(k_F)^{-1}$. So if we compare the average kinetic energy $E_K = k_F^2/2m \sim r_0^{-2}$, and the potential energy $E_V \sim e^2/(4\pi r_0) \sim r_0^{-1}$, $E_V/E_K \sim r_0 \ll 1$, so the high density condition is equivalent to the requirement of weak-scattering condition, so that the perturbation theory is well applied. In most metals, the single-particle approximation explains many of their low energy properties.

Next we apply the Hartee-Fock approximation on Eq. 16:

$$H^{HF} = \sum_{\mathbf{k}} E^{HF}(\mathbf{k}) c_{\mathbf{k}}^+ c_{\mathbf{k}} + const. \tag{17}$$

$$E^{HF}(\mathbf{k}) = E^0(\mathbf{k}) + \sum_{\mathbf{k}'}[V(0) - V(\mathbf{k}-\mathbf{k}')]n_{\mathbf{k}'} = E^0(\mathbf{k}) + NV(0) - \sum_{\mathbf{k}'} n_{\mathbf{k}'} V(\mathbf{k}-\mathbf{k}') \tag{18}$$

(Hartee term is zero for the jellium model, but we still keep it here for the general case.) The second term is the interaction with the average electron charge.

This (always negative) contribution to the total energy of the electron liquid is known as the exchange energy.

For a non-interacting system, a pair of electrons with the same spin orientation are affected by the antisymmetry of the wave function: the pair correlation function for same-spin electrons, $g(r)$ vanishes for $r \to 0$ and tends to 1 for $r \to \infty$. The depletion region at small separations is precisely the "exchange hole", and its existence leads to the negative exchange energy.

Then we take electronic density $n(\mathbf{k})$ as a functional, we can construct the energy functional as

$$E[n(\mathbf{k})] = \sum_{\mathbf{k}} E^{HF}(\mathbf{k}) n(\mathbf{k}) = \sum_{\mathbf{k}}[E^0(\mathbf{k})n(\mathbf{k}) + NV(0)n(\mathbf{k})] - \sum_{\mathbf{k},\mathbf{k}'} n(\mathbf{k})n(\mathbf{k}')V(\mathbf{k}-\mathbf{k}') \tag{19}$$

Performing the Fourier transformation, we get

$$\sum_k E_k\Theta(E_F-E_k)=\int dx\sum_k\phi_k^*(x)[-\frac{\nabla^2}{2m}+U(x)]\phi_k(x)\Theta(E_F-E_k)+$$
$$\int dx\delta(x-z)\int dzV(x-z)\sum_k\sum_j|\phi_j(z)|^2\Theta(E_F-E_j)\phi_k^*(x)\phi_k(x)\Theta(E_F-E_k)$$
$$-\int dx\int dzV(x-z)\sum_k\sum_j\phi_k^*(x)\phi_k(z)\phi_j(z)^*\phi_j(x)\Theta(E_F-E_j)\Theta(E_F-E_k) \quad (20)$$

By taking variation on the wave function $\phi_k(x)$, we reach the self-consistent equations for the the eigenfunctions. We obtain the self-consistent Hartee-Fock equation as (j,k is the band index):

$$[-\frac{\nabla^2}{2m}+U_0(x)]\phi_k(x)+\int dzV(x-z)\delta(x-z)\sum_j|\phi_j(z)|^2\Theta(E_F-E_j)\phi_k(x)$$
$$-\int dzV(x-z)\sum_j\phi_k(z)\phi_j(z)^*\Theta(E_F-E_j)\phi_j(x)=E_k\phi_k(x) \quad (21)$$

Since charge density is $n(x)=\sum_j|\phi_j(x)|^2\Theta(E_F-E_j)$, the first term is $\int dzV(x-z)n(z)$, which is Hartee field as a local direct potential that is proportional to the particle density. The second term describes the exchange effect, which is a static but non-local effect.

Eq. 21 constitute a very complicated problem: An initial set of single-particle wave functions and energies are assumed know,.then Eq. 21 becomes a one-body eigenvalue equation that determines a new set of eigenfunctions and eigenvalues. This process is continued until a self-consistent solution is obtained for both $\{\phi_j(x),E_j\}$. The above self-consistent equations are first derived by Hartee 1928 and Fock 1930.

Exchange energy of free electron gas. Let us look at the self-consistent Hartee-Fock equation Eq. 21. The set of energies and wave functions $\{E_k,\phi_k(x)\}$ should be solved numerically. Here we can estimate the exchange energy using unperturbative wavefunctions.

Eq. defines the energies:

$$
\begin{aligned}
&E_{kin}+E_{Hartee}+E_{xc}=E_{tot}\\
&E_{kin}=\sum_k\int dx\phi_k^*(x)[-\frac{\nabla^2}{2m}+U(x)]\phi_k(x)\Theta(E_F-E_k)\\
&E_{Hartee}=\int dx\delta(x-z)\int dzV(x-z)\sum_{k,j}|\phi_j(z)|^2\Theta(E_F-E_j)\phi_k^*(x)\phi_k(x)\Theta(E_F-E_k)\\
&E_{xc}=-\int dx\int dzV(x-z)\sum_{k,j}\phi_k^*(x)\phi_k(z)\phi_j(z)^*\phi_j(x)\Theta(E_F-E_j)\Theta(E_F-E_k)\\
&E_{tot}=\sum_k E_k\Theta(E_F-E_k)
\end{aligned}
\tag{22}
$$

If we make a rough approximation, $\phi_k(x)=\phi_k^0(x)$, by setting the wave function as the unperturbative ones, we can get (this is equivalent to reduce from self-consistent Hartee-Fock to Hartee-Fock approximation)

$$
\begin{aligned}
E_{xc}&=-\int dx\int dzV(x-z)\sum_{k,j}(\phi_k^0(x))^*\phi_k^0(z)(\phi_j^0(z))^*\phi_j^0(x)\Theta(E_F-E_j)\Theta(E_F-E_k)\\
&=-\int dx\int dz\frac{4\pi e^2}{|x-z|}\frac{1}{\sqrt{V}^4}\sum_{\mathbf{k},\mathbf{p}}e^{i\mathbf{k}\cdot\mathbf{x}}e^{-i\mathbf{k}\cdot\mathbf{z}}e^{i\mathbf{p}\cdot\mathbf{z}}e^{i\mathbf{p}\cdot\mathbf{x}}\Theta(E_F-E_p)\Theta(E_F-E_k)\\
&=-\frac{1}{V}\sum_{\mathbf{k},\mathbf{p}}\frac{4\pi e^2}{|\mathbf{k}-\mathbf{p}|^2}\Theta(E_F-E_p)\Theta(E_F-E_k)\equiv\sum_{\mathbf{k}}\Sigma_{xc}(k)\Theta(E_F-E_k)
\end{aligned}
$$

where we define

$$
\begin{aligned}
\Sigma_{xc}(k)&=-\frac{1}{V}\sum_{\mathbf{p}}\frac{4\pi e^2}{|\mathbf{k}-\mathbf{p}|^2}\Theta(E_F-E_k)=-\int\frac{d^3p}{(2\pi)^3}\frac{4\pi e^2}{|\mathbf{k}-\mathbf{p}|^2}\Theta(E_F-E_p)\\
&=-\frac{e^2}{\pi}\int_0^{k_F}p^2dp\int_{-1}^1\frac{dt}{k^2+p^2-2kpt}=-\frac{e^2}{\pi k}\int_0^{k_F}pdp\ln|\frac{k+p}{k-p}|\\
&=-\frac{e^2k_F}{\pi}[1+\frac{1-y^2}{2y}\ln|\frac{1+y}{1-y}|]
\end{aligned}
\tag{23}
$$

and $y=k/k_F$. Then ,

$$
\begin{aligned}
E_{xc}&=\sum_{\mathbf{k}}\Sigma_{xc}(k)\Theta(E_F-E_k)\\
&=-V\frac{e^2k_F}{\pi}\frac{k_F^3}{2\pi^2}\int_0^1y^2dy[1+\frac{1-y^2}{2y}\ln|\frac{1+y}{1-y}|]=-V\frac{3e^2k_F}{4\pi}\frac{k_F^3}{3\pi^2}
\end{aligned}
\tag{24}
$$

So the exchange energy per electron is:

$$
\epsilon_{xc}=\frac{E_{xc}}{N_e}=-\frac{3e^2k_F}{4\pi}=-\frac{3}{4}(\frac{3}{\pi}n)^{1/3}
\tag{25}
$$

and number of electrons are

$$N_e = 2\frac{V}{(2\pi)^3}\int d^3p\Theta(E_F - E_p) = 2\frac{V}{(2\pi)^3}2\pi\int_0^{k_F} p^2dp\int_{-1}^{1} dt = V\frac{k_F^3}{3\pi^2} \tag{26}$$

APPLICATION: DENSITY FUNCTIONAL THEORY

At this step, we could discuss the connection with the famous density-functional theory (DFT), based on the knowledge about hte Hartee-Fock approximation. In history, a fundamental progress in DFT is the Kohn-Sham equations (1965), which provides the first practical and calculable framework in DFT. Here we briefly discuss it. The Kohn–Sham equations consist of non-interacting particles in a potential that is analogous to the Hartee-Fock approximation as listed above.

Kohn-Shan proposed an auxiliary system of independent "electrons" that can be derived from the solution of independent-particle equations with some as-yet-undetermined potential $V_{eff}(\mathbf{r})$:

$$[-\frac{1}{2m}\nabla^2 + V_{eff}(\mathbf{r})]\phi_i(\mathbf{r}) = E_i\phi_i(\mathbf{r}) \tag{27}$$

with auxiliary eigenvalues E_i and eigenvectors $\phi_i(\mathbf{r})$. The condition of minimum energy (or self-consistency) for fixed particle number yields the effective potential

$$V_{eff}(\mathbf{r}) = U(\mathbf{r}) + V_H(n(\mathbf{r})) + V_{xc}(n(\mathbf{r})) \tag{28}$$

where the density is given by

$$n(\mathbf{r}) = \sum_i n_F(E_F - E_i)|\phi_i(\mathbf{r})|^2. \tag{29}$$

The Hartee potential is $\int dzV(x-z)n(z) = \int d\mathbf{r}'\frac{n(\mathbf{r}')}{|\mathbf{r}-\mathbf{r}'|}$, that is the same what we obtained in Eq. 21. The exchange term is intrinsically non-local, and its form needs special care. Propose that we already know some form of exchange potential $V_{xc}(n(\mathbf{r}))$ (we will discuss it later), we can using Eq. 27 28 29 to make a self-consist loop to do the calculations. At the solution, $V_{eff}(n(\mathbf{r})) = V_{KS}(n(\mathbf{r}))$ is the Kohn–Sham potential that (except for an irrelevant additive constant) is in one-to-one correspondence with the density n.

Hohenberg and Kohn Theorem 1. *The ground-state of a many-electron system is a functional of the electron density (i.e. two ground state wave functions must be identical if the expectation values of the density operator are identical for these wave functions).* That is, there is a one-to-one correspondence between the ground state wave function and its density expectation value.

Proof. Let $|\Psi\rangle, |\Psi'\rangle$ be two different many-body wave functions which are the ground states for different external potentials V_{eff} and V'_{eff}, and $\langle\Psi|n(r)|\Psi\rangle = \langle\Psi'|n(r)|\Psi'\rangle$. Then

$$E' = \langle\Psi'|H'|\Psi'\rangle < \langle\Psi|H'|\Psi\rangle = \langle\Psi|H|\Psi\rangle + \langle\Psi|(H'-H)|\Psi\rangle = E + \langle\Psi|V'-V|\Psi\rangle \quad (30)$$

The inequality is introduced into the above relations by the variational theorem because $|\Psi\rangle$ is not the ground state of H'. Interchanging primed and unprimed quantities in the above relation leads to a similar inequality,

$$E < E' + \langle\Psi|V-V'|\Psi\rangle \quad (31)$$

and combining the two inequalities leads to

$$E' + E < E + E' + [\langle\Psi|V-V'|\Psi\rangle + \langle\Psi|V'-V|\Psi\rangle] \quad (32)$$

Using the fact that $|\Psi\rangle$ and $|\Psi'\rangle$ have the same density, the terms in the brackets cancel out (see the Hartee-Fock energy potential), leaving us with the contradiction

$$E' + E < E + E' \quad (33)$$

Therefore the assumption that the two states have the same density must be incorrect. The theorem follows. (Note that this line of argument assumes that the ground state is non-degenerate.)

Hohenberg and Kohn Theorem 2. *The ground state energy may be expressed as a functional of the density and this functional is minimized by the true ground state density.*

The accomplishment of Hohenberg and Kohn (1964) was to show that the energy can also be considered to be a functional of the density $E_{HK}[n]$. And then one can deduce that, the correlation potential $E_{xc}[n] = [E_{HK}[n] - T_{ind}[n] - E_H[n]]$ (T_{ind} is kinetic energy from inde-

pendent electrons, E_H is Hartee energy), only depends on the local density $n(\mathbf{r})$. (therefore exchange potential is $V_{xc} = \frac{\delta}{\delta n} E_{xc}(n)$) However, it still remains to find good approximations for the unknown exchange–correlation contribution. The reason DFT is so successful is that even very simple approximate functionals can be remarkably accurate for groundstate properties of many systems. One widely used approximation is, the local density approximation (LDA). The exchange–correlation energy density is supposed to depend locally on the charge density, $E_{xc}^{LDA} = \int d\mathbf{r} n(\mathbf{r}) \epsilon_{xc}(n(\mathbf{r}))$, and $\epsilon_{xc}(n) = -\frac{3}{4}(\frac{3}{\pi}n)^{1/3}$ (see Eq. 25). This is from the averaged exchange energy of high-density (non-interacting) electron gas. LDA only applies to some weakly correlated systems like simple metals.

Furthermore, the discussion of Hartee-Fock can help us understand many techniques in the DFT. Different methods assume differnt form of exchange potential $V_{xc} = \delta n \delta E_{xc}(n)$, i.e. try to find different ways to deal with correlation effect. Let me briefly summarize them here:

- LDA.— The LDA approximation is, in principle, adequate for system with a low spatial varying electron density, but it revealed good for a wider variety of materials: $E_{xc}^{LDA} = \int dr n(r) E_{xc}[n(r)], E_{xc}[n] = -\frac{3}{4}(\frac{3}{\pi}n)^{1/3}$.

- GGA/PBE.— Expanding V_{xc} in terms of the gradient of the density in order to account for the non-homogeneity of the true electron density. This allows corrections based on the changes in density away from the coordinate. These expansions are referred to as generalized gradient approximations for exchange and correlation: $E_{xc}^{GGA} = \int dr n(r) E_{xc}(n(r); \nabla n(r))$. PBE is a special GGA [J. P. Perdew, K. Burke, and M. Ernzerhof, Phys. Rev. Lett. 77, 3865 (1996)].

- Hybrid functionals.— Hybrid functionals are a class of approximations to the exchange-correlation energy functional in DFT that incorporate a portion of exact exchange from Hartree-Fock theory with the rest of the exchange-correlation energy from other sources (ab initio or empirical).

  PBE0. The PBE0 functional mixes the PBE exchange energy and Hartree-Fock exchange energy in a set 3 : 1 ratio, along with the full PBE correlation energy: $E_{xc}^{PBE0} = \frac{1}{4} E_x^{HF} + \frac{3}{4} E_x^{PBE} + \frac{1}{4} E_c^{HF}$.

HSE. The HSE (Heyd-Scuseria-Ernzerhof) exchange-correlation functional uses an error-function-screened Coulomb potential to calculate the exchange portion of the energy in order to improve computational efficiency, especially for metallic systems: $E_{xc}^{HSE} = aE_x^{HF;SR}(\omega) + (1-a)E_x^{PBE;SR}(\omega) + E_x^{PBE;LR} + E_c^{PBE}$, where a is a mixing parameter and is an adjustable parameter controlling the short-rangeness of the interaction.

- GW.— The GW approximation is an approximation made in order to calculate the self-energy of a many-body system of electrons. The approximation is that the expansion of the self-energy Σ in terms of the single particle Green's function G and the screened Coulomb interaction W [L. Hedin, Phys. Rev. 139, 796-823 (1965)]. The screened Coulomb interaction can be expressed by $W(q) = V(q)/\epsilon(q)$. where $\epsilon(q)$ is the dielectric function.

- DMFT.— A non-perturbative way is used to calculate the self-energy function. Please see the future lectures.

APPLICATION: TOPOLOGICAL MOTT INSULATOR ON THE HONEYCOMB LATTICE

The lattice model under consideration for spinless (spin-polarized) fermions takes the form

$$H_{\text{spinless}} = -t\sum_{\langle i,j\rangle} c_i^\dagger c_j + V_1\sum_{\langle i,j\rangle} n_i n_j + V_2\sum_{\langle\langle i,j\rangle\rangle} n_i n_j + V_3\sum_{\langle\langle\langle i,j\rangle\rangle\rangle} n_i n_j. \tag{34}$$

Here, $c_i^{(\dagger)}$ annihilates (creates) a spinless fermion on site i and $n_i = c_i^\dagger c_i$ is the fermion density operator on site i. The sums run over nearest-neighbor $\langle i,j\rangle$, second-neighbor $\langle\langle i,j\rangle\rangle$, or third-neighbor bonds $\langle\langle\langle i,j\rangle\rangle\rangle$. The hopping amplitude is denoted by t and the parameters V_1, V_2, and V_3 quantify the nearest-neighbor, second-neighbor and third-neighbor repulsion, respectively.

The model for spinful fermions includes an additional on-site repulsive interaction U. The Hamiltonian reads

$$H_{\text{spinful}} = -t\sum_{\langle i,j\rangle} c_{i\sigma}^\dagger c_{j\sigma} + U\sum_i n_{i\uparrow}n_{i\downarrow} + V_1\sum_{\langle i,j\rangle} n_i n_j + V_2\sum_{\langle\langle i,j\rangle\rangle} n_i n_j + V_3\sum_{\langle\langle\langle i,j\rangle\rangle\rangle} n_i n_j. \tag{35}$$

Here, $c_{i\sigma}^{(\dagger)}$ annihilates (creates) a fermion on site i with spin $\sigma =\uparrow,\downarrow$, $n_{i\sigma} = c_{i\sigma}^\dagger c_{i\sigma}$ and $n_i = \sum_\sigma n_{i\sigma}$. The summing convention and the meaning of the parameters V_1, V_2, and V_3 are the same as for the spinless model.

The model Hamiltonian for spinless fermions with nearest-neighbor and next-nearest neighbor interactions is written as

$$\begin{aligned} H = &-\sum_{\langle ij\rangle} t\left(c_i^\dagger c_j + h.c.\right) + V_1\sum_{\langle i,j\rangle}(n_i-1)(n_j-1) \\ &+V_2\sum_{\langle\langle i,j\rangle\rangle}(n_i-1)(n_j-1) - \mu\left(\sum_i n_i - N\right) \end{aligned} \tag{36}$$

where V_1 and V_2 are nearest-neighbor and next-nearest-neighbor interaction strengths, respectively.

Since the honeycomb lattice is bipartite, consisting of two triangular sublattices (referred to here as A and B), nearest-neighbor repulsion will favor a charge density wave (CDW) phase with an order parameter $\rho = \frac{1}{2}\left(\langle c_{iA}^\dagger c_{iA}\rangle - \langle c_{iB}^\dagger c_{iB}\rangle\right)$ that is consistent with overall charge conservation and describes a phase with a broken discrete (inversion) symmetry.

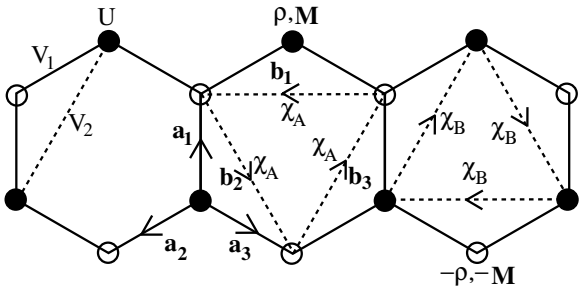

FIG. 1: Interactions considered in our model Hamiltonian (left-most hexagon), Eq. 36. Various order parameters are shown for the A-sublattice (open circles) in the middle hexagon and for the B-sublattice (filled circles) in the right-most hexagon. The CDW order parameter ρ is a real scalar, SDW order parameter $\boldsymbol{M}$ a real vector and the QAH/QSH order parameters χ_A, χ_B are complex 4-vectors. In the case of spinless fermions, χ_A, χ_B are complex scalars. χ_A, χ_B are both defined on the directed second neighbor links defined by $\boldsymbol{b}_i$.

However, since the second neighbor interactions within a sublattice are frustrated, CDW order will be suppressed; instead we consider the possibility of orbital ordering by defining the following order parameter for i, j next nearest neighbors: $\chi_{ij} = \chi^*_{ji} = \langle c^\dagger_i c_j \rangle$. Let $\boldsymbol{a}_1, \boldsymbol{a}_2, \boldsymbol{a}_3$ be the nearest-neighbor displacements from a B-site to an A-site such that $\boldsymbol{z} \cdot \boldsymbol{a}_1 \times \boldsymbol{a}_2$ is positive. We also define the displacements $\boldsymbol{b}_1 = \boldsymbol{a}_2 - \boldsymbol{a}_3$, $\boldsymbol{b}_2 = \boldsymbol{a}_3 - \boldsymbol{a}_1$, etc, which connect two neighboring sites on the same sublattice (Fig. 1). A translational and rotational invariant ansatz of χ_{ij} is chosen as

$$\chi_{i,i+\mathbf{b}_s} = \begin{cases} \chi_A = |\chi| e^{i\phi_A}, \ i \in A \\ \chi_B = |\chi| e^{i\phi_B}, \ i \in B \end{cases} \tag{37}$$

which are *complex* scalars that live along the directed second neighbor links.

Let's decouple the terms one by one:

$$\begin{aligned} V_1 \sum_{\langle ij \rangle} n_i n_j &= V_1 \sum_{\langle ij \rangle} ((\langle n \rangle + \rho) n_{jB} + n_{iA}(\langle n \rangle - \rho) - (\langle n \rangle^2 - \rho^2)) \\ V_2 \sum_{\langle\langle i,j \rangle\rangle} n_i n_j &= V_2 \sum_{\langle\langle i,j \rangle\rangle} -c^\dagger_i c_j \chi_{ij} + h.c. + \chi^*_{ij} \chi_{ij} \end{aligned} \tag{38}$$

Owing to translational symmetry, the mean-field free energy at $T = 0$ is readily obtained:

$$F\left(\rho, \chi, \bar{\phi}, \phi\right) = -\sum_{\boldsymbol{k}} \sqrt{|t(\boldsymbol{k})|^2 + \left(V_1 \rho + 2V_2 |\chi| S_{\boldsymbol{k}+\bar{\phi}} S_\phi\right)^2} + 3L^2 \left(V_1 \rho^2 + 2V_2 |\chi|^2\right) \tag{39}$$

We have defined the following quantities: $t(\boldsymbol{k}) = \sum_{n=1}^{3} \exp(i\boldsymbol{k}\cdot a_n)$, $\bar{\phi} = (\phi_A + \phi_B)/2, \phi = (\phi_A - \phi_B)/2, S_{\boldsymbol{k}+\bar{\phi}} = \sum_{n=1}^{3} \sin\left(\boldsymbol{k}\cdot b_n + \bar{\phi}\right), S_\phi = \sin\phi$. Thus, the next-neighbor hopping amplitudes are purely real only when both $\phi = 0$ and $\bar{\phi} = 0$.

To see the mean field energy, we explain details as below. With the help of Eq. 38, we have the mean-field Hamiltonian as

$$\begin{aligned}
H &= \sum_k \gamma_k c^\dagger_{k,A} c_{k,B} + h.c. + V_1 \sum_k (\langle n\rangle + \rho) c^\dagger_{k,B} c_{k,B} + (\langle n\rangle - \rho) c^\dagger_{k,A} c_{k,A} \\
&= (c^\dagger_{k,A}, c^\dagger_{k,B}) \begin{pmatrix} \xi_{k,A} + (\langle n\rangle - \rho) & t_k \\ t^\dagger_k & \xi_{k,B} + (\langle n\rangle + \rho) \end{pmatrix} \begin{pmatrix} c_{k,A} \\ c_{k,B} \end{pmatrix} \\
t_k &= e^{i\vec{k}\cdot\vec{a}_1} + e^{i\vec{k}\cdot\vec{a}_2} + e^{i\vec{k}\cdot\vec{a}_3} \\
\xi_{k,A} &= \chi e^{i\phi_A + i\vec{k}\cdot\vec{b}_1} + \chi e^{-i\phi_B - i\vec{k}\cdot\vec{b}_2} + ... = 2\chi \sum_{n=1}^{3} \cos(\phi_A + \vec{k}\cdot\vec{b}_n) \\
\xi_{k,B} &= 2\chi \sum_{n=1}^{3} \cos(\phi_B + \vec{k}\cdot\vec{b}_n)
\end{aligned}$$

Thus, mean-field energy is obtained by the equation

$$(E_k - (\xi_{k,A} - \rho))(E_k - (\xi(k,B) + \rho) - |t_k|^2) = 0$$

and

$$E_k = \frac{\xi_{k,A} + \xi_{k,B}}{2} \pm \sqrt{|t_k|^2 + [V_1\rho + 2\chi V_2 S_{k+\bar{\phi}} S_\phi]^2}$$

Please note that $\frac{1}{2}(\xi_{k,A} - \xi_{k,B}) = -2\chi S_{\vec{k}+\bar{\phi}} S_\phi$.

When both ρ and $\chi = 0$, and at half-filling, the system remains a semi-metal consisting of two Fermi points $\boldsymbol{K}_\pm$ which obey $\boldsymbol{K}_\pm \cdot \boldsymbol{b}_i = \pm 2\pi/3$ and the density of states vanishes linearly; the dispersion in the vicinity of these so called Dirac points is governed by a 2D massless Dirac Hamiltonian in $\boldsymbol{k}$-space . The CDW phase corresponds to an ordinary insulator with a gap at the Fermi energy. As for the order parameter χ, which describes the second-neighbor hopping, its *phase* relative to the nearest neighbor hopping amplitude plays an important role in determining its properties: while a non-zero $Re(\chi)$ merely shifts the energy of the Dirac points, a non-zero imaginary part $Im(\chi)$ *opens a gap* at the Fermi points. Thus, when the system remains at half-filling, it is more favorable to develop purely imaginary next-neighbor hopping amplitudes; such a configuration corresponds to a phase with *spontaneously broken time-reversal symmetry.*

To see whether such a phase can be favored, we minimize the free-energy and arrive at the following self-consistent equations:

$$\frac{\partial F}{\partial \rho} = 0 \Rightarrow \rho = \frac{1}{2L^2}\sum_{\boldsymbol{k}} \frac{V_1\rho + 2V_2\chi S_{\boldsymbol{k}+\bar{\phi}} S_\phi}{\sqrt{|t(\boldsymbol{k})|^2 + \left(V_1\rho + 2V_2\chi S_{\boldsymbol{k}+\bar{\phi}} S_\phi\right)^2}} \tag{40}$$

$$\frac{\partial F}{\partial \chi} = 0 \Rightarrow \chi = \frac{S_\phi}{6L^2}\sum_{\boldsymbol{k}} \frac{S_{\boldsymbol{k}+\bar{\phi}}\left(V_1\rho + 2V_2\chi S_{\boldsymbol{k}+\bar{\phi}} S_\phi\right)}{\sqrt{|t(\boldsymbol{k})|^2 + \left(V_1\rho + 2V_2\chi S_{\boldsymbol{k}+\bar{\phi}} S_\phi\right)^2}} \tag{41}$$

When $\chi = 0$, it is easy to see from the first equation above that CDW order develops continuously at a critical value V_{1c} given by

$$\frac{1}{V_{1c}} = \frac{1}{2L^2}\sum_{\boldsymbol{k}} \frac{1}{|t(\boldsymbol{k})|}, \tag{42}$$

Due to the vanishing density of states (DOS) near the Fermi points, there is no instability towards CDW formation with infinitesimal interactions. Interestingly, the self-consitent equation for χ shows that a non-trivial self-consistent solution can only occur when $\phi \neq 0$; a detailed investigation of these equations show that when $V_1 = 0$, beyond a critical value of $V_{2c} > 0$, which satisfies

$$\frac{1}{V_{2c}} = \frac{1}{3L^2}\sum_{\boldsymbol{k}} \frac{S^2_{\boldsymbol{k}+\bar{\phi}}}{|t_{\boldsymbol{k}}|}, \tag{43}$$

a phase in which $|\chi| > 0$,$\bar{\phi} = 0$, and $\phi = \pm\pi/2$ is favored. Such a phase is also stable at finite V_1 and is thus does not require fine-tuning (see Fig. 2). In this phase, the system acquires purely imaginary second-neighbor hoppings with a chirality which is determined by the sign of ϕ.

We have obtained the complete phase diagram in the $V_1 - V_2$ plane; within mean-field theory, there is a continuous transition from the semi-metal to either the CDW or the QAH phase and there is also a first-order transition from the CDW to the QAH phase. By integrating out the fermionic fields, it is possible to construct a Landau-Ginzburg (LG) theory expansion near the nodal region where the order parameters are vanishingly small. Due to the linear dispersion of the Fermi points, the LG free-energy contains anomalous terms of the form $|\rho|^3$ and $|Im(\chi)|^3$ arising from linear dispersion in the vicinity of the Fermi points. The significance of such terms is that even within mean-field theory, the CDW order parameter, for instance, grows as $(V_1 - V_{1c})$ rather than the usual $(V_1 - V_{1c})^{1/2}$. Furthermore, the Landau-Ginzburg theory describing the competition between the CDW

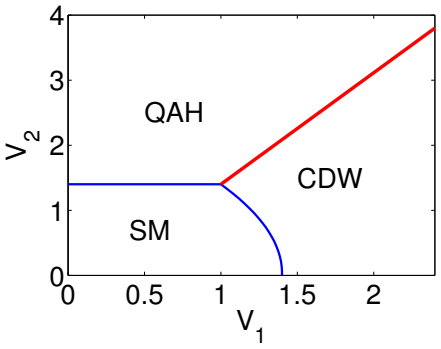

FIG. 2: Phase diagram for spinless fermions ($t = 1$) [2]. The semi-metallic (SM) state that occurs at weak-coupling is separated from the CDW and the topological QAH states via a continuous transition (blue curve). The line separating the QAH and CDW marks a first-order transition (shown in red), which terminates at a bi-critical point.

and QAH phases confirms the existence of the first order line between these two phases that terminates in the bicritical point leading into the semimetal phase.

APPLICATION: THE HUBBARD MODEL

The Hubbard model was named after John Hubbard (in 1963), which is the simplest model of interacting particles in a lattice. The main motivation was to tackle the behaviour of correlated (rather than non-interacting) electrons in solids, describing the transition between conducting and insulating systems. It contains only two terms in the Hamiltonian: a kinetic term allowing for tunneling ("hopping") of particles between sites of the lattice and a potential term consisting of an on-site interaction. The particles can either be fermions, as in Hubbard's original work, or bosons, when the model is referred to as either the "Bose–Hubbard model".

Hamiltonian in the simplest case of non-degenerate band, with one orbital per site, can be expressed in the second-quantization formalism as:

$$\hat{H} = \sum_{i,j} t_{ij,\sigma} c^{\dagger}_{i,\sigma} c_{j,\sigma} + h.c. + U \sum_{i} n_{i\uparrow} n_{i\downarrow} \tag{44}$$

where we denote the creation operator $c^{\dagger}_{i\sigma}$ for an electron of spin σ in the orbital at lattice site i. t_{ij} is the amplitude of the process, the so-called hopping amplitude from site j, where the electron is destroyed, to site i, where the electron is created. The term t_{ij} is the traduction in the second-quantization language of both the kinetic energy and the crystal-potential energy associated with an electron at site:

$$t_{ij,\sigma} = \int d\vec{r} \varphi^{*}_{\vec{R}_i,\sigma}(\vec{r}) \left(-\frac{\hbar^2 \nabla^2}{2m} + V(\vec{r}) \right) \varphi_{\vec{R}_j,\sigma}(\vec{r}) \tag{45}$$

where wannier wave-functions $\varphi_{\vec{R}_i,\sigma}(\vec{r})$ are centered at site $\vec{R}_i$. We suppose that the hopping amplitude does not depend on the spin variable and therefore we drop the σ label. The term $V(\vec{r})$ represents the periodic crystal potential energy. As stated above, one approximation that is usually employed for the hopping term t_{ij} is to consider it different from zero only when i and j are nearest-neighbour sites ($t_{ij} = t$), as their overlap is usually the largest.

Operators $\hat{n}_{i\sigma} \equiv \hat{c}^{\dagger}_{i\sigma} \hat{c}_{i\sigma}$ count the number of particles at site i with spin σ. They are projection operators, ie, $\hat{n}^2_{i\sigma} = \hat{n}_{i\sigma}$ (either there is one electron with spin σ at site i or there are no electrons). The expectation value $\langle \hat{n}_{i\sigma} \rangle \equiv \langle \Psi_0 | \hat{n}_{i\sigma} | \Psi_0 \rangle$ in the many-body ground-state $|\Psi_0\rangle$ represents the electron density $n_{i\sigma}$ at site i with spin σ (mean occupation number). The physical origin of $\hat{H}_U$ is the Coulomb repulsion of the electrons: when at site i both spin-up and spin-down electrons are present, from Eq. (1) they contribute to the total energy with a

term $+U$, as both $\hat{n}_{i\uparrow}$ and $\hat{n}_{i\downarrow}$ in $\hat{H}_U$ give one. If, on the other side, the two electrons belong to two separate atoms, they do not feel any Coulomb repulsion (this is of course a strong constraint). Formally, the on-site Coulomb repulsion can be written as:

$$U = \frac{e^2}{4\pi\varepsilon_0} \int d\vec{r} d\vec{r} \left|\varphi_{\vec{R}_i,\sigma}(\vec{r})\right|^2 \frac{1}{\left|\vec{r} - \vec{r}\,'\right|} \left|\varphi_{\vec{R}_i,\bar{\sigma}}(\vec{r}\,')\right|^2 \tag{46}$$

The Coulomb term does not depend on the site-label i, if we suppose the system homogeneous. Notice that in the extreme limit $\mathrm{U/t} = 0$, we recover a purely band-like (tight-binding) picture, with just kinetic energy and crystal periodic potential, and in the opposite limit $\mathrm{t/U} = 0$, we find a purely atomic picture.

The Hubbard model was proposed to describe electrons in 3d transition metals. In these elements, the radial wave function of the 3d-electrons has a very small spatial extent. Therefore, when the 3d shell is occupied by several electrons, these are forced to be close to one another on the average so that the electrostatic energy is large. Initially, the model was introduced to provide an explanation for the itinerant ferromagnetism of transition metals, such as iron and nickel, but the past 50 years have seen its relevance go far beyond that original context.

The simplicity of the Hubbard model, when written down, is deceptive. Not only had Gutzwiller, Kanamori and Hubbard already extracted different physics from the model, it turned out to be a 'mathematically hard' problem: an exact solution has so far only been obtained for the one-dimensional case. Today, with ever-increasing computer power, numerical simulations of the model are mainstream — particularly when trying to get a grip on the role of the topology of the underlying lattice, a 'hidden variable' indeed.

Ever since its inception, the model has spawned new lines of research in theoretical physics; the development of dynamical mean-field theory is a noteworthy example. Although the model quickly became a firm favourite of theorists, it twice experienced a sudden rise in popularity due to breakthroughs in experimental physics.

The first followed the discovery of high-temperature superconductors in 1986. Until then, the Hubbard model was believed to have little to do with superconductivity. However, in the wake of the high-temperature superconductivity 'revolution', one particular adaptation of Hubbard's original model called the t–J model (originally arising in the context of doped Mott–Hubbard insulators) emerged as a compelling candidate for hosting a superconducting state. A rigorous proof of the existence (or non-existence) of a superconducting ground state

in the t–J model is still missing — underlining that research on superconductivity and the Hubbard model is continuing.

A second boost in activity surrounding the Hubbard model came in the 2000s, when the field of cold-atom optical trapping had advanced so far that experimental realizations of the Hubbard model could be achieved. A landmark experiment demonstrated how a lattice of bosonic atoms displays a transition from a superfluid to a Mott insulator, a result accounted for by the Bose–Hubbard model (the Hubbard model for bosons). Many other variants of the Hubbard model, including the original model for fermions, have been experimentally realized by now, a development that nicely illustrates how a model can become the target of experiments itself — and, more generally, how theoretical and experimental physics can entangle and spark further progress.

Part of the legacy of Hubbard's model is that it launched the field of strongly correlated systems — it is undoubtedly the archetypal model of many-body physics. Although the Hubbard model secured it's place in (condensed-matter) physics textbooks many decades ago, it is very likely that it will continue to play an important role in fundamental research as well. In particular, the continuing experimental progress in artificial lattices of cold atoms and superconductivity, where the Hubbard model and its modifications play a prominent role, should be a stimulus for further explorations.

Conduction limit $U \to 0$

The two-dimensional square lattice is drawn in figure 3. The unit-cell is spanned by the 2 vectors $\vec{a}_1$ and $\vec{a}_2$, of common length a. However, for our calculations we consider the cell of double area spanned by the 2 vectors $\vec{b}_1$ and $\vec{b}_2$, with the idea of looking for possible antiferromagnetic ground-states. Such a cell encloses two atomic sites that can in principle be inequivalent (e.g., spin $\uparrow$ and spin $\downarrow$). In what follows, we adopt the site-label $\vec{R}_i$ for the double unit cell and, within each cell, the two atoms are labeled by an extra index $\alpha = 1, 2$. For example, as shown in figure 3, nearest neighbours of $\alpha = 1$ sites are necessarily $\alpha = 2$ and vice-versa (bipartite lattice). The general creation (annihilation) operator for an electron at site $\vec{R}_i$, position α, spin σ can be written as: $\hat{c}^\dagger_{i\alpha\sigma}$ ($\hat{c}_{i\alpha\sigma}$).

In spite of the cumbersome form, the meaning of hopping terms is quite straightforward: the first line represents the four nearest-neighbour hopping energies (represented by dashed

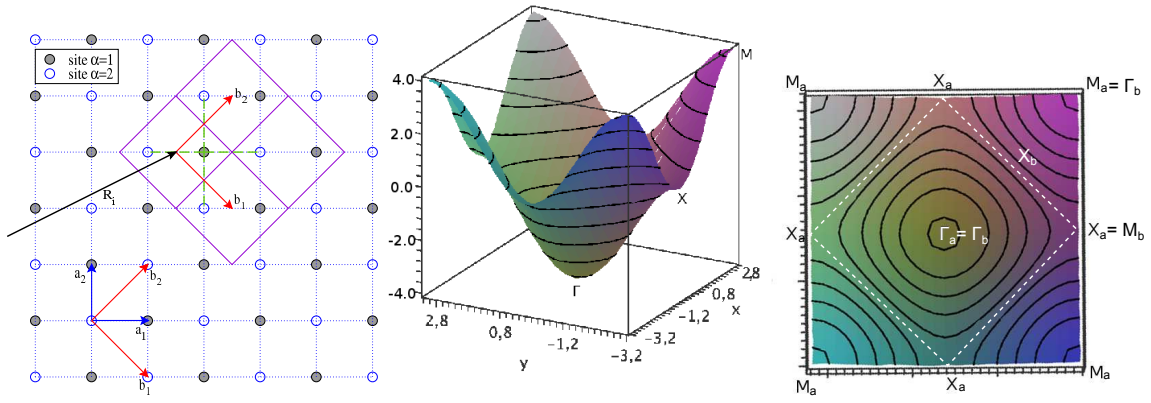

FIG. 3: Double ($\vec{b}_1$,$\vec{b}_2$) cells for the square lattice. Nearest neighbours of $\alpha = 1$, $\vec{R}_i$ are highlighted by the green dashed lines. The four violet cells represent nearest-neighbour cells in the ($\vec{b}_1$,$\vec{b}_2$)-basis. Band structure in tight-binding approach ($U = 0$). Full band-structure for the single cell. A Van-Hove singularity (the white dashed line which connects the X_a points) appears at half filling.

green lines in figure 3) when site $\vec{R}_i$ is of $\alpha = 1$-type and site $\vec{R}_j$ is of $\alpha = 2$-type, and the second line the opposite case. As we employ the reciprocal lattice of the ($\vec{b}_1$,$\vec{b}_2$) direct lattice, we must express the nearest neighbours in terms of linear combinations of $\vec{b}_1$, $\vec{b}_2$ vectors.

Consider first the hopping part of the Hamiltonian, $\hat{H}_{\tilde{t}}$. By inserting the $\vec{k}$-transformed operators, we get the usual tight-binding band structure:

$$\begin{aligned}
\hat{H}_{\tilde{t}} &= -\frac{1}{N}\sum_{ij\alpha\alpha'\sigma} t_{ij}^{\alpha\alpha'} \sum_{\vec{k}\vec{k}'} e^{-\imath\vec{k}\cdot\vec{R}_i}\hat{c}^{\dagger}_{\vec{k}\alpha\sigma} e^{\imath\vec{k}'\cdot\vec{R}_j}\hat{c}_{\vec{k}'\alpha'\sigma} \\
&= -\frac{1}{N}\sum_{\vec{k}\vec{k}'\alpha\alpha'\sigma} \hat{c}^{\dagger}_{\vec{k}\alpha\sigma}\hat{c}_{\vec{k}'\alpha'\sigma} \sum_{ij} t_{ij}^{\alpha\alpha'} e^{-\imath\vec{k}\cdot\vec{R}_i} e^{\imath\vec{k}'\cdot\vec{R}_j} \\
&= -\sum_{\vec{k}\vec{k}'\alpha\alpha'\sigma} \hat{c}^{\dagger}_{\vec{k}\alpha\sigma}\hat{c}_{\vec{k}'\alpha'\sigma} \sum_{j} t_{\vec{\eta}_j}^{\alpha\alpha'} e^{\imath\vec{k}'\cdot\vec{\eta}_j} \frac{1}{N}\sum_{i} e^{-\imath(\vec{k}-\vec{k}')\cdot\vec{R}_i} \\
&= \sum_{\vec{k}\alpha\alpha'\sigma} \hat{c}^{\dagger}_{\vec{k}\alpha\sigma}\hat{c}_{\vec{k}\alpha'\sigma}\varepsilon_{\vec{k}}^{\alpha\alpha'}
\end{aligned} \tag{47}$$

where we defined the matrix hamiltonian in the α-α' basis as: $\varepsilon_{\vec{k}}^{\alpha\alpha'} = -\sum_j t_{\vec{\eta}_j}^{\alpha\alpha'} e^{\imath\vec{k}\cdot\vec{\eta}_j}$. In passing from the second to the third line of we used the translational invariance of the structure factor $t_{ij}^{\alpha\alpha'}$: this means that if we write $\vec{R}_j = \vec{R}_i + \vec{\eta}_{ij}$, the vectors $\vec{\eta}_{ij}$, and therefore the way of counting nearest neighbours, are independent of the starting point $\vec{R}_i$. So, we can write: $\vec{\eta}_{ij} \to \vec{\eta}_j$. Moreover we used the fact that $\frac{1}{N}\sum_i e^{-\imath(\vec{k}-\vec{k}')\cdot\vec{R}_i} = \delta_{\vec{k}\vec{k}'}$.

As we have two atoms per unit cell, the matrix hamiltonian is a 2×2 matrix ($\alpha,\alpha'=1,2$) that should be diagonalized in order to have the band structure $\varepsilon^{\pm}_{0\vec{k}}$. From the explicit expression of the structure constants, we get the matrix:

$$H_{\tilde{t}} = \begin{bmatrix} 0 & t\gamma_{\vec{k}} \\ t\gamma^{*}_{\vec{k}} & 0 \end{bmatrix} \tag{48}$$

where $\gamma_{\vec{k}} = -\left\{1 + e^{-i\vec{k}\cdot(\vec{b}_1+\vec{b}_2)} + e^{-i\vec{k}\cdot\vec{b}_1} + e^{-i\vec{k}\cdot\vec{b}_2}\right\}$. Its diagonalisation leads to two bands given by:

$$\varepsilon^{\pm}_{0\vec{k}} = \pm t|\gamma_{\vec{k}}| = \pm t\left|2\cos\left(\vec{k}\cdot\frac{\vec{b}_1+\vec{b}_2}{2}\right) + 2\cos\left(\vec{k}\cdot\frac{\vec{b}_2-\vec{b}_1}{2}\right)\right| \tag{49}$$

The band structure and density of states (DOS) per unit cell are depicted in figure, together with those for the single cell ($\vec{a}_1$,$\vec{a}_2$), for comparison. Bandwidth is $W = 8t$. At half-filling, we have a nested Fermi surface, leading to a van Hove logarithmic singularity in the DOS. We remind that nesting is the property by which any point of the Fermi surface is related to another point of the Fermi surface by a fixed vector, in this case the vector $(\pi/a, \pi/a)$, because the Fermi surface is a square at half-filling, as shown in figure 1. Clearly, at this level, changing the choice of the unit cell (a pure convention) does not change our results: in fact, the second band is just the folding of the first band of the single cell, as can be also seen by considering that $\frac{\vec{b}_1+\vec{b}_2}{2} = \vec{a}_1$ and $\frac{\vec{b}_2-\vec{b}_1}{2} = \vec{a}_2$. This comes from the fact that the point $M_a \equiv (\pi/a, \pi/a)$ in the reciprocal cell of the direct cell ($\vec{a}_1$,$\vec{a}_2$) becomes equivalent to $\Gamma_b \equiv (0,0)$ in the reciprocal cell of the direct cell ($\vec{b}_1$,$\vec{b}_2$).

Atomic limit $U \to \infty$

At half filling case, we have one electron at each lattice site exactly, whose energy is zero. The ground state has large degeneracy. $|\uparrow\uparrow ...\rangle$ all have the same energy.

In this case, $[H, n_i] = 0$ for each j, so that the eigenstates of H are also eigenstates of all the individual number operators. The number operators also commute with each other, so basic principles of quantum and statistical mechanics tell us we can consider each term in H on its own. We thus arrive at a single site model which is very easily solved. (Since all sites are independent, we drop the site index in this limit.)

We have four possibilities corresponding to the site being empty $|0\rangle$ having a up fermion or down spin fermion $|\uparrow(\downarrow)\rangle$, or being doubly occupied. $|\uparrow\downarrow\rangle$. Each of these is an eigenstate of H with eigenvalues U, 0, 0, respectively.

Interaction terms U

The presence of $\hat{H}_{\tilde{U}}$, changes these simple results even at a mean-field level. We remind that the mean-field approximation corresponds to neglecting the fluctuations around the mean density. Such fluctuations are defined as $\Delta\hat{n}_{i\alpha\sigma} \equiv \hat{n}_{i\alpha\sigma} - \langle\hat{n}_{i\alpha\sigma}\rangle$, i.e., the difference between the exact number operator $\hat{n}_{i\alpha\sigma}$ and the mean occupation number $\langle\hat{n}_{i\alpha\sigma}\rangle$. From this relation, we get: $\hat{n}_{i\alpha\sigma} \equiv \langle\hat{n}_{i\alpha\sigma}\rangle + \Delta\hat{n}_{i\alpha\sigma}$. If we suppose homogeneity of the system, then $\langle\hat{n}_{i\alpha\sigma}\rangle$ is independent of the cell position $\vec{R}_i$, and we can drop the label i and write:

$$\begin{aligned}\hat{n}_{i\alpha\uparrow}\hat{n}_{i\alpha\downarrow} &= [\Delta\hat{n}_{i\alpha\uparrow} + \langle\hat{n}_{\alpha\uparrow}\rangle]\cdot[\Delta\hat{n}_{i\alpha\downarrow} + \langle\hat{n}_{\alpha\downarrow}\rangle] \\ &= \Delta\hat{n}_{i\alpha\uparrow}\Delta\hat{n}_{i\alpha\downarrow} + \sum_{\sigma}\hat{n}_{i\alpha\sigma}\langle\hat{n}_{\alpha\bar{\sigma}}\rangle - \langle\hat{n}_{\alpha\uparrow}\rangle\langle\hat{n}_{\alpha\downarrow}\rangle\end{aligned} \tag{50}$$

In a mean-field approximation we can neglect the first term of the previous equation, quadratic in the fluctuations. This implies that $\hat{H}_{\tilde{U}}$ becomes:

$$\hat{H}_{\tilde{U}}^{\mathrm{MF}} = \underbrace{U\sum_{i\alpha\sigma}\hat{n}_{i\alpha\sigma}\langle n_{\alpha\bar{\sigma}}\rangle}_{\hat{H}_U} \underbrace{- UN\sum_{\alpha}\langle n_{\alpha\uparrow}\rangle\langle n_{\alpha\downarrow}\rangle}_{E_U} \tag{51}$$

The second term E_U is a constant for given magnetic configuration and number of particles, as it does not depend on creation or annihilation operators but only on their average values. However, it must be integrated in the calculation of the magnetic phase diagram, as such a term advantages paramagnetic configurations with respect to ferromagnetic and antiferromagnetic (E_U is negative and the product $\langle n_{\alpha\uparrow}\rangle\langle n_{\alpha\downarrow}\rangle$, for fixed number of particles per site, is maximum when $\langle n_{\alpha\uparrow}\rangle = \langle n_{\alpha\downarrow}\rangle$).

By using the Fourier transform, the first term of (51) becomes: $\tilde{H}_U = U\sum_{i\alpha\sigma}\langle n_{\alpha\bar{\sigma}}\rangle\hat{c}^{\dagger}_{i\alpha\sigma}\hat{c}_{i\alpha\sigma} = U\sum_{\vec{k}\alpha\sigma}\langle n_{\alpha\bar{\sigma}}\rangle\hat{c}^{\dagger}_{\vec{k}\alpha\sigma}\hat{c}_{\vec{k}\alpha\sigma}$, diagonal in α. Therefore the energy per $\vec{k}$-point for a spin-σ electron is obtained by diagonalizing the 2x2 matrix:

$$\begin{bmatrix} U\langle n_{1\bar{\sigma}}\rangle & t\gamma_{\vec{k}} \\ t\gamma^{*}_{\vec{k}} & U\langle n_{2\bar{\sigma}}\rangle \end{bmatrix} \tag{52}$$

Where $\gamma_{\vec{k}}$ has been defined after (48). This Hamiltonian can be easily diagonalized analytically, as the associated eigenvalue problem leads to the second-order algebraic equation for the eigenenergies $\varepsilon^{\pm}_{\vec{k}}$:

$$\varepsilon^2_{\vec{k}} - \varepsilon_{\vec{k}}\left(U\langle n_{1\bar{\sigma}}\rangle + U\langle n_{2\bar{\sigma}}\rangle\right) + U^2\langle n_{1\bar{\sigma}}\rangle\langle n_{2\bar{\sigma}}\rangle - t^2|\gamma_{\vec{k}}|^2 = 0 \tag{53}$$

The solutions of this second-order equation provide the mean-field band-energies per $\vec{k}$-point for a spin-σ electron, once we add again the term E_U (divided by N, because $\varepsilon_{\vec{k}}$ is the energy per spin-σ electron):

$$\begin{aligned}
\varepsilon^{\pm}_{\vec{k}\sigma} &= U\left(\frac{\langle n_{1\bar{\sigma}}\rangle + \langle n_{2\bar{\sigma}}\rangle}{2}\right) - U\big(\langle n_{1\uparrow}\rangle\langle n_{1\downarrow}\rangle + \langle n_{2\uparrow}\rangle\langle n_{2\downarrow}\rangle\big) \\
&\pm \frac{1}{2}\sqrt{U^2(\langle n_{1\bar{\sigma}}\rangle - \langle n_{2\bar{\sigma}}\rangle)^2 + 16t^2\left(\cos\left[\vec{k}\cdot\tfrac{\vec{b}_1+\vec{b}_2}{2}\right] + \cos\left[\vec{k}\cdot\tfrac{\vec{b}_1-\vec{b}_2}{2}\right]\right)^2} \\
&= U\left(\frac{\langle n_{1\bar{\sigma}}\rangle + \langle n_{2\bar{\sigma}}\rangle}{2}\right) - U\big(\langle n_{1\uparrow}\rangle\langle n_{1\downarrow}\rangle + \langle n_{2\uparrow}\rangle\langle n_{2\downarrow}\rangle\big) \\
&\pm \frac{1}{2}\sqrt{U^2(\langle n_{1\bar{\sigma}}\rangle - \langle n_{2\bar{\sigma}}\rangle)^2 + 4(\varepsilon^{\pm}_{0\vec{k}})^2}
\end{aligned} \tag{54}$$

From the last line we see that $\hat{H}^{MF}_{\tilde{U}}$ contributes to the total energy as a density-dependent and spin-dependent (because of $\bar{\sigma}$) renormalization of the tight-binding energy $\varepsilon^{\pm}_{0\vec{k}}$. This double dependence on the density and on the spin is at the basis of the richness in the phase diagram shown in figure 6, allowing to get paramagnetic (PM), ferromagnetic (FM) and antiferromagnetic (AFM) phases.

Computational details.

In order to find the ground-state energy for a given magnetic configuration, we need to employ a self-consistent scheme as, for a given spin σ, the energy depends on the mean occupation number of opposite spin, $\langle \hat{n}_{\alpha\bar{\sigma}}\rangle$, which in turns depends on the eigenvectors of the energy matrix itself. As shown in figure 4, we therefore start from a given configuration of input parameters, we follow steps 3, 4, 5 and 6, up to the self-consistency condition expressed in frames 7 and 8, and finally move back to frame 2 or end to frame 9, depending on whether the condition is not satisfied or satisfied, respectively. The condition is satisfied when the output occupation number is the same as the input occupation number within a threshold that we fixed to 10^{-5}.

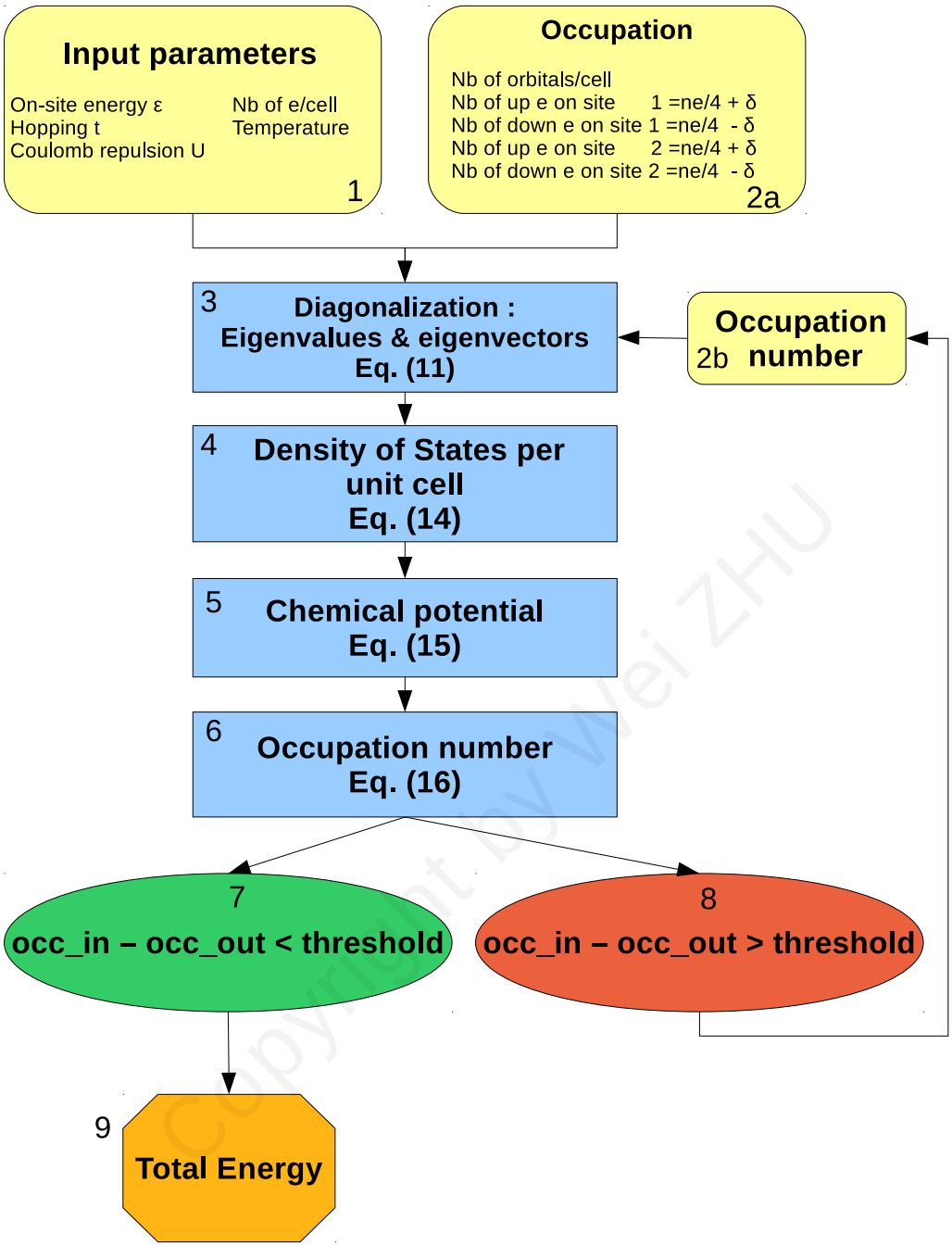

FIG. 4: Scheme of the self-consistent algorithm leading to the ground-state phase diagram of figure 6. Equations are described in the text

In more details, we proceeded as follows: for practical reasons we found it simpler to

numerically diagonalize the Hamiltonian of (52) through the Lapack libraries (frame 3), in order to determine eigenvalues $\varepsilon_{j\sigma}(\vec{k})$ and eigenvectors $|\Psi^j_{\vec{k}\sigma}\rangle = \sum_\alpha A^j_{\alpha,\sigma}(\vec{k})|\alpha\vec{k}\rangle$ (with $j = 1, 2$). We actually work with the chemical potential in order to fix the particle density aposteriori: $\hat{H}^\mu_H = \hat{H}_H - \mu \sum_{i\alpha\sigma} \hat{n}_{i\alpha\sigma}$. The calculations performed in frames 4, 5 and 6 are based on equations (55), (56) and (57) given below. The first of these equations expresses the DOS per unit cell, $\rho(\varepsilon)$:

$$\rho(\varepsilon) = \frac{1}{N} \sum_{\vec{k},j,\sigma} \delta \left[\varepsilon - \varepsilon_{j\sigma}(\vec{k}) \right] \tag{55}$$

The Dirac delta function in (55) is numerically calculated through a Gaussian function whose broadening is optimized after a convergence study: if the width of the Gaussian is too wide compared to the step between two energy points in ε, the DOS is too smooth, whereas if the width is too narrow, artificial oscillations appear. A more elegant approach might be to use the Methfessel-Paxton method, usually implemented in more advanced packages for electronic structure calculations.

As a second step we determine the chemical potential μ by the implicit equation:

$$\int_{-\infty}^{+\infty} d\varepsilon \, \rho(\varepsilon) \frac{1}{\exp[\beta(\varepsilon - \mu)] + 1} = n_e \tag{56}$$

Here $\beta = 1/k_B T$ is the Boltzmann factor and we have defined the total number of electrons per unit cell: $n_e \equiv \sum_{\alpha,\sigma} \langle n_{\alpha\sigma} \rangle$. Finally, the average number of particles per site α and per spin σ at a given temperature T is given by:

$$\langle n_{\alpha\sigma} \rangle = \frac{1}{N} \sum_{\vec{k},j=1,2} |A^j_{\alpha,\sigma}(\vec{k})|^2 \frac{1}{\exp[\beta(\varepsilon_{j\sigma}(\vec{k}) - \mu)] + 1} \tag{57}$$

At finite temperature, the thermodynamic variable to minimize is of course not the total energy, E, but the free energy, $F = E - TS$, what implies a calculation of the entropy of the system, through the equation:

$$S(T) = -k_B \int_{-\infty}^{\infty} d\varepsilon \rho(\varepsilon) \Big\{ f(\varepsilon) \ln[f(\varepsilon)] \, + \, [1 - f(\varepsilon)] \ln[1 - f(\varepsilon)] \Big\} \tag{58}$$

Here $f(\varepsilon)$ is the Fermi-Dirac distribution. However, in what follows, we are interested in the ground-state phase diagram of the model, i.e., at $T = 0$. We minimized therefore the total energy and used the parameter T of equations (56) and (57) for convergence purposes only. It is in fact common practice to use a Fermi-Dirac distribution, characterized by a

parameter T different from zero, even in the $T \to 0$ limit, in order to smooth the step function that appears in equations (56) and (57) for $T = 0$.

In general, we computed the total energy for each magnetic phase as a function of t/U. A phase transition is then characterized by the crossing of two (or more) free-energy curves: for example, we have represented the magnetic free energy as a function of t/U in figure 5 for a specific occupation number ($n = 0.8$), in order to highlight a magnetic (AFM/FM) transition. In this case the phase transition from AFM to FM phase is obtained at $t/U = 0.13$, value at which the total FM energy becomes smaller than the AFM energy.

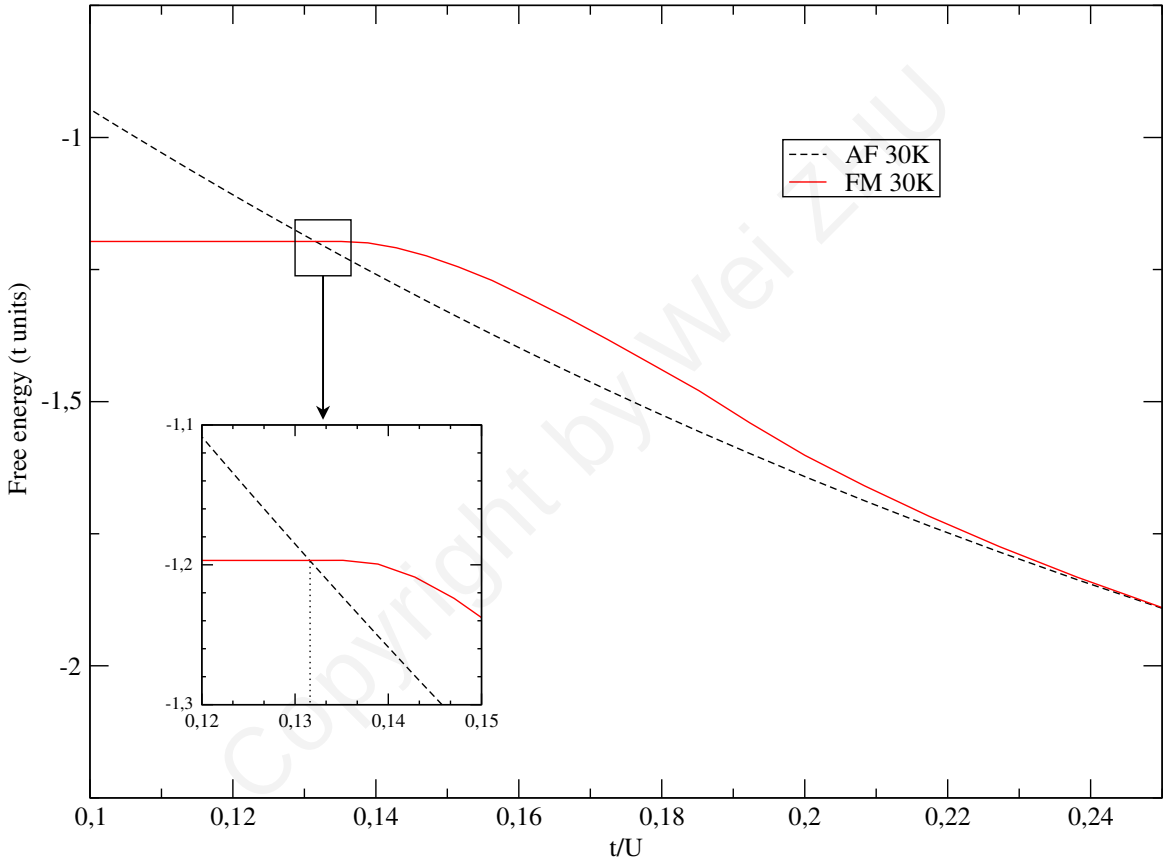

FIG. 5: A phase transition occurs where magnetic-energy curves cross each other. For n=0.8 the system becomes ferromagnetic below $t/U = 0.13$. We have chosen an inverse temperature $\beta \sim 0.003$ eV.

Discussion of results: phase diagram.

In figure 6, we have drawn the band structures for both FM and AFM phases to highlight the differences with the PM case. FM bands are shifted rigidly with respect to PM bands by about $\pm U\delta n$, where δn is half the spin unbalance (see below). AFM bands are instead characterized by the opening of a gap that can be related to the difference $U(|\langle n_{1\bar{\sigma}}\rangle - \langle n_{2\bar{\sigma}}\rangle|)$ in (54). This gap leads to an insulating phase for $n_e = 2.0$. It is important to notice that such a gap is not related to a metal-insulator transition (MIT) of the Mott-Hubbard kind, as it is not related to the electronic correlations (that are absent by definition in a mean-field calculation), but to magnetism. This MIT is rather called Slater MIT, in honor of J.C. Slater that foresaw it in 1951. In fact, differently from Mott that did not originally ascribed his MIT to magnetic interactions, Slater thought that the origin of the metal-to- insulator transition was determined by the onset of AFM long-range order, exactly as in the scheme described in the present paper. Therefore a Slater insulator is characterized by a band gap determined by a superlattice modulation of the magnetic periodicity. This is not the case of a Mott insulator.

Our main result is the ground-state phase diagram, drawn in Figure 6 as a function of the number of electrons per site and of t/U. Such a phase diagram had been already obtained in the literature in 1985 by Hirsch, though in a different context and without providing all the details of the derivation that can be found here. As a general feature the phase diagram shows a clear symmetry around half filling, i.e., one electron per site, where antiferromagnetism is the lowest-energy configuration. This symmetry had to be expected, since it is a symmetry of the Hubbard hamiltonian for nearest-neighbour hopping. Far from half-filling, paramagnetism is advantaged by a high value of t/U, whereas a low value of t/U leads instead to ferromagnetism. This tendency for the PM/FM phases can be easily understood: the ground-state of n non-interacting electrons ($U = 0$) is PM because the minimum-energy constraint in combination with the Pauli principle forces to fill all the energy levels from the lowest ($\varepsilon_{\min}$) to the highest (μ) with an equal number of $n/2$ up and $n/2$ down electrons. In the opposite extreme case, for $U/t \to \infty$, the system can gain energy by a total magnetization (say, all electrons with spin up), in order to minimize the energy term $U\langle n_{\downarrow}\rangle$. In the intermediate t/U cases, only the numerical study of equations (52), (55), (56) and (57) can provide us with the magnetic phase of the system.

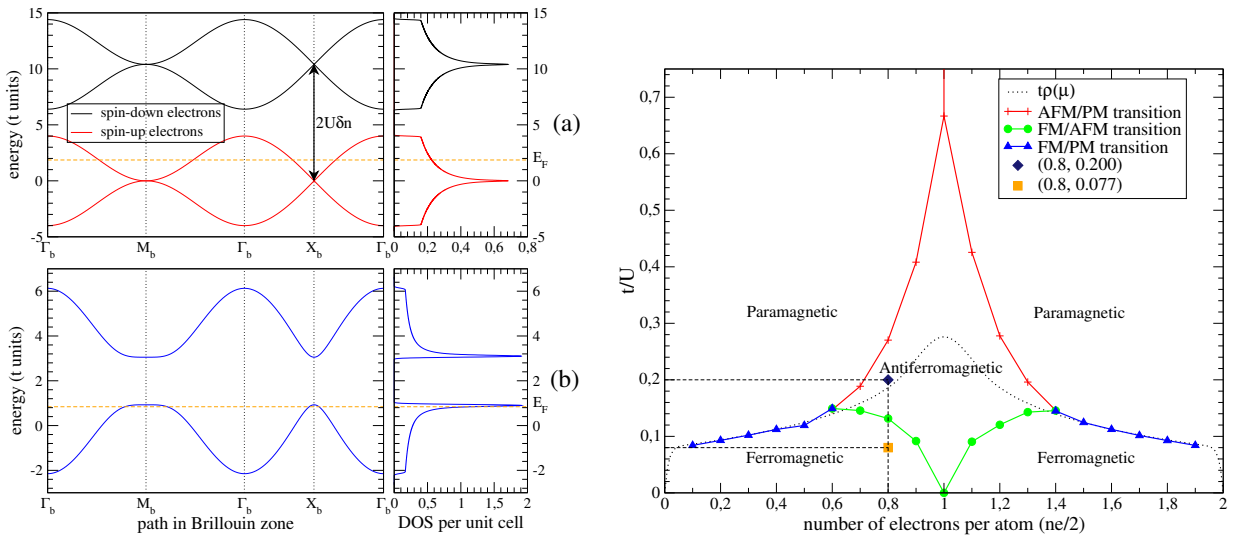

FIG. 6: Ground-state phase diagram of the Hubbard model on a square lattice as a function of the ratio t/U and of the electron filling. The physical relevance of the curve $t\rho(\mu)$ is detailed in the text. We used an inverse-temperature value $\beta = 0.03t$ in the equations. Band structure and DOS for: (a) FM configuration: $t/U = 0.077$; $n_e = 1.6$ ($n_{1\uparrow} = n_{2\uparrow} = 0.8$ and $n_{1\downarrow} = n_{2\downarrow} = 0$) and (b) AFM configuration: $t/U = 0.2$; $n_e = 1.6$ ($n_{1\uparrow} = n_{2\downarrow} = 0.62$ and $n_{1\downarrow} = n_{2\uparrow} = 0.18$). In the FM case the exchange splitting is $2U\delta n$. In the AFM case a Slater gap appears, leading to an insulator for $n_e = 2.0$. The DOS has been obtained by modeling equation (55) with a normalized Gaussian of width 0.05 t and with a 500×500 k-point grid.

There exists however a criterion that allows us to foresee the stability of the PM phase versus the FM phase just on the base of the two parameters U and $\rho(\mu)$, the DOS at the Fermi energy ($\varepsilon_F = \mu$ at $T = 0$). This is Stoner criterion. The mean field solution is found by minimization, which gives the self-consistency equations $H_{MF} = \sum_k [\xi_k + U\langle n_{\bar\sigma}\rangle] c^\dagger_{k\sigma} c_{k\sigma} + const.$. We obtain at zero temperature. $\langle n_{\bar\sigma}\rangle = \int_0^{E_F} \rho(E)dE \sim \int dE\sqrt{E} = E_F^{3/2} \sim k_F^3$, where the fermi momentum is determined by $\hbar^2 k^2_{F\sigma}/2m + U\langle n_{\bar\sigma}\rangle = \mu$. Thus, we have

$$\hbar^2\langle n_\uparrow\rangle^{3/2}/2m + U\langle n_\downarrow\rangle = \mu, \quad \hbar^2\langle n_\downarrow\rangle^{3/2}/2m + U\langle n_\uparrow\rangle = \mu \tag{59}$$

The solutions have three different regime depending on U: normal state ($\langle n_\uparrow\rangle = \langle n_\downarrow\rangle$), partial magnetism ($\langle n_\uparrow\rangle < \langle n_\downarrow\rangle$), and ferromagnetism ($\langle n_\uparrow\rangle = 0, \langle n_\downarrow\rangle = 1$)

The original Stoner criterion for ferromagnetic stability is:

$$U\rho(\mu) \geq 1 \tag{60}$$

Equation 60 can also be written as $\frac{t}{U} \leq t\rho(\mu)$. The corresponding equality, that marks the phase transition, has been reproduced in figure 6. All our calculated points for the PM/FM transition lie on the theoretical curve $\frac{t}{U} = t\rho(\mu)$ represented by a dotted line in Figure 6. We infer from the Stoner criterion that a ferromagnetic instability is expected in materials showing a high density of states at Fermi level. This is indeed the case for Fe, Co and Ni. It is also possible to find a similar criterion for the AFM/PM and AFM/FM transitions, but its derivation is technically more involved because it is based on a Bogoliubov transformation. This leads to a gap-equation formally equivalent to the one of the BCS theory of superconductivity.

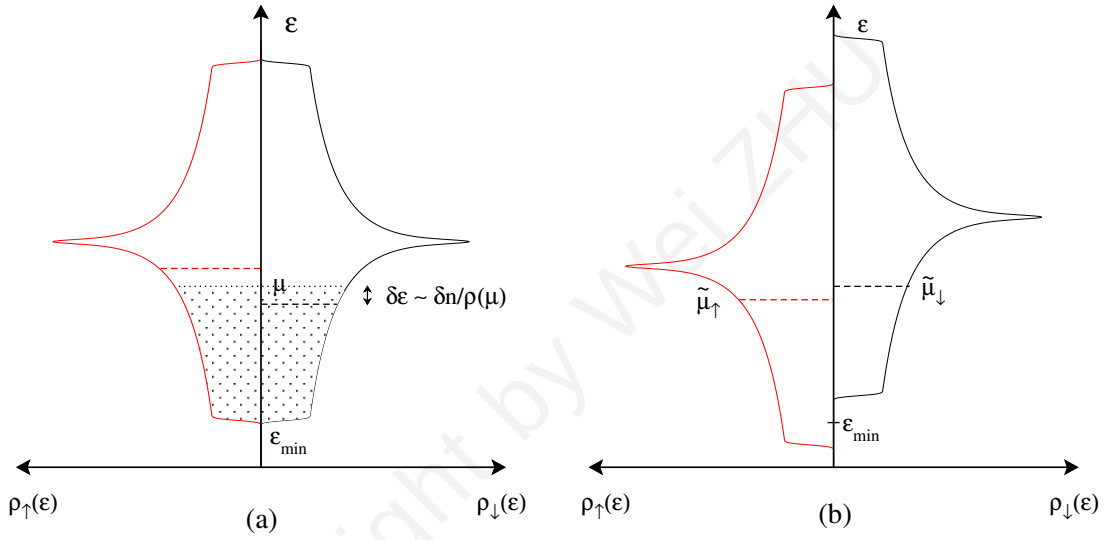

FIG. 7: (a) If $\delta n \ll n$ spin-down electrons are moved to spin-up DOS, for $U = 0$, this leads to a shift of the chemical potential $\pm\delta\varepsilon \sim \pm\delta n/\rho(\mu)$: PM state is always favored. (b) If $U \neq 0$, then spin-up DOS is lowered in enegy by $-U\delta n + U(\delta n)^2/n$ and spin down DOS is raised in energy by $U\delta n + U(\delta n)^2/n$. Therefore, depending on $\rho(\mu)$, FM stability can be obtained for sufficiently high U (see text).

Generalizations and conclusion.

In the previous section we have analyzed formalism and phase diagram of the one-band Hubbard model on a square lattice in the mean-field approximation. For completeness, in this section we give a brief overview of four possible generalizations of the model to provide

the link to the more advanced literature, with applications to real materials.

The first modification that can be dealt with concerns the application to a different lattice. This primarily leads to a different DOS than the one shown in figure, thereby modifying quantitatively, but not necessarily qualitatively, the phase diagram. The fact that quantitative changes in the DOS do not necessarily imply qualitative (topological) modifications of the phase diagram. Qualitatively similar behavior is also obtained in all cases where bipartite lattices are considered, as the honeycomb lattice. We remind that a lattice is called bipartite if two atoms of kinds A and B can be accommodated in it in such a way that any atom of kind A is only surrounded by atoms of kind B and vice-versa. On the contrary, qualitatively and quantitatively different results are obtained in the case of frustrated lattices, like the triangular lattice. This is the case because antiferromagnetic interactions can be depleted by geometrical frustrations and paramagnetism is generally advantaged in lattices that are not bipartite.

As a second modification, it is possible to extend the hopping term beyond nearest neighbours. For example next-nearest-neighbour hopping is not necessarily zero as supposed in the present paper. In the square lattice such a term corresponds to an hopping integral between the two atoms along the directions of $\vec{b}_1$ and $\vec{b}_2$ of figure 3. The effect of this term in the DOS of a square lattice is to remove the nesting property of Fermi surface at half filling. For a 2-dimensional square lattice such a calculation in the mean-field approximation has been performed, who indeed found a deformed phase diagram with respect to that of figure 6, without the symmetry around half-filling.

In third place, instead of 2-dimensional systems we could move to 3-dimensional lattices. In the case of a cubic lattice, for example, this leads to the removal of the van Hove singularity, determined by the 2-dimensional square-lattice topology with nearest neighbours, and therefore to the removal of the logarithmic singularity at half-filling in the DOS. All these modifications can of course be combined together, to get a final phase diagram that can be substantially different from the one presented in this paper even in the mean-field approximation.

One final modification that applies to realistic systems, is to introduce multi-orbital Hubbard models and/or multi-band Hubbard models. Models where d or f orbitals are introduced belong to the first kind. In this case a further index m up to 5 for d orbitals and up to 7 for f orbitals must be introduced to deal with electron creation and annihilation

operators for different wave-functions (e.g., d_{xy}, d_{yz}, $d_{x^2-y^2}$, etc.). Hopping terms are then modified in a similar way as when we moved from (1) to (4). However, the extra labels, α, α' in (4) and m, m' in (61) below have different physical interpretations, m, m' representing two different d or f (or sometimes p) orbitals on the same atom. The multiorbital Hubbard hamiltonian is:

$$H = \sum_{ijmm'\sigma} t_{ij}^{mm'} \hat{c}_{im\sigma}^{\dagger} \hat{c}_{jm'\sigma} + \sum_{imm'\sigma\sigma'} U^{mm'} \hat{n}_{im\sigma} \hat{n}_{im'\sigma'}$$
$$+ J \sum_{m \neq m'} \left(\hat{c}_{im\uparrow}^{\dagger} \hat{c}_{im\downarrow}^{\dagger} \hat{c}_{im'\downarrow} \hat{c}_{im'\uparrow} - \hat{c}_{im\uparrow}^{\dagger} \hat{c}_{im\downarrow} \hat{c}_{im'\downarrow}^{\dagger} \hat{c}_{im'\uparrow} \right) \tag{61}$$

It is important to underline that in this case, several intra-atomic Coulomb terms appear, depending on whether intra-orbital ($U^{mm'}$, with $m = m'$) or inter-orbital ($U^{mm'}$, with $m \neq m'$) Coulomb repulsion is concerned. Moreover, because of the multi-dimensional orbital degree of freedom, also Hund's exchange J appears, for $m \neq m'$. Interestingly, this implies the appearence of an exchange term in the mean-field approximation: the Hartree approximation of this paper would become an Hartree-Fock approximation.

Finally, multi-band Hubbard models are those where several atomic species are present, not all necessarily characterized by the same Hubbard U (that can also be zero in some cases). Probably the most famous of this kind are the Anderson periodic model, used to describe the interaction of a localised electron (e.g. an f electron) with a 'Fermi sea', or the pd-model used to describe CuO_2-planes in superconducting cuprates, where 2 kinds of p bands and 1 d band are introduced.

This rapid oveview shows the potential applications that the generalisation of a simple mean-field solution of the Hubbard model can have. We would like to stress, again, that many of these generalisations are not just academic exercises and can bring the interested student very close to real researches in condensed-matter physics. At the same time, based on our experience, we found out that the calculations and the physical concepts presented in this paper are in average understood by graduate students. Last but not least, the self-consistent numerical procedure used in section 4 to diagonalise the hamiltonian and find the phase diagram can represent a useful tool for students to make the link between formal implicit formulas and the way useful figures have to be derived.

APPLICATION: TWISTED GRAPHENE/TMD SYSTEMS

Previously, we mainly focus on the single orbital/band calculation for simplicity. But in many cases the physical problems are complex which involve many orbitals/bands. Here we would like to discuss such a case.

Recently, motivated by the experimental progresses in twisted graphene and TMD (e.g. MoTe2), it is very popular to theoretically study using the Hartee-Fock approximation. Here we just briefly discuss it.

The low energy physics of a single particle(electron/hole) near the single-layer K valley in the twisted graphene/$MoTe_2$ can be described by the continuum model

$$H_0 = \sum_{n,\sigma,\mathbf{k}} h_{n\sigma\mathbf{k}} \hat{d}^\dagger_{n,\sigma,\mathbf{k}} \hat{d}_{n,\sigma,\mathbf{k}}, \tag{62}$$

$\hat{d}^\dagger_{n\sigma\mathbf{k}}$ creates a hole in the Bloch eigenstate of $h_{n\sigma k}$ with subband index n, spin/valley σ and momentum $\mathbf{k}$ in the moiré Brillouin zone (BZ). It is stress that, the physics in the moiré BZ is related to the original BZ as

$$\hat{d}^\dagger_{n,\sigma,\boldsymbol{k}} = \sum_{\alpha,\boldsymbol{G}} u_{\alpha,\boldsymbol{G};n}(\boldsymbol{k}) \hat{c}^\dagger_{\alpha,\boldsymbol{k}+\boldsymbol{G}} \tag{63}$$

where the momentum of $\hat{c}^\dagger$ operator is defined in the original (BZ) of the graphene/TMD while the momentum of the operator $\hat{d}^\dagger$ is defined in the moiré BZ (mBZ) (see the discussion before), with the periodic boundary condition $\hat{d}^\dagger_{\boldsymbol{k}+\boldsymbol{G};n} = \hat{d}^\dagger_{\boldsymbol{k};n}$ and denote $\hat{d}^\dagger_{\{\boldsymbol{k}+\boldsymbol{G}\};n} := \hat{d}^\dagger_{\boldsymbol{k};n}$. α is the sublattice index, $\boldsymbol{G}$ is the reciprical vector. The wave function reads

$$\psi_n(\boldsymbol{k}) = \sum_{\alpha,\boldsymbol{G}} u_{\alpha,\boldsymbol{G};n}(\boldsymbol{k}) e^{i\boldsymbol{r}\cdot(\boldsymbol{k}+\boldsymbol{G})} \tag{64}$$

Next we define $\tilde{\boldsymbol{k}}_1, \tilde{\boldsymbol{k}}_2, \tilde{\boldsymbol{q}} \in$ BZ and $\boldsymbol{k}_1, \boldsymbol{k}_2, \boldsymbol{k}_3, \boldsymbol{k}_4, \boldsymbol{q} \in$ mBZ, satisfing $\tilde{\boldsymbol{k}}_1 = \boldsymbol{k}_1 + \boldsymbol{G}_1$,

$\tilde{\boldsymbol{k}}_2 = \boldsymbol{k}_2 + \boldsymbol{G}_2$ and $\tilde{\boldsymbol{q}} = \boldsymbol{q} + \boldsymbol{G}$. The two-body interaction reads

$$\begin{aligned}
\hat{H}^{\text{int}} =& \frac{1}{2N_s} \sum_{\alpha\alpha'} \sum_{\tilde{\boldsymbol{k}}_1 \tilde{\boldsymbol{k}}_2 \tilde{\boldsymbol{q}}} V_{\alpha\alpha'}(\tilde{\boldsymbol{q}}) \hat{c}^\dagger_{\alpha,\tilde{\boldsymbol{k}}_1+\tilde{\boldsymbol{q}}} \hat{c}^\dagger_{\alpha',\tilde{\boldsymbol{k}}_2-\tilde{\boldsymbol{q}}} \hat{c}_{\alpha',\tilde{\boldsymbol{k}}_2} \hat{c}_{\alpha,\tilde{\boldsymbol{k}}_1} \\
=& \frac{1}{2N_s} \sum_{\alpha\alpha',\boldsymbol{k}_{1-4},\boldsymbol{G}_{1-4},n_{1-4}} \delta_{\boldsymbol{k}_4+\boldsymbol{G}_4,\boldsymbol{k}_1+\boldsymbol{G}_1+(\boldsymbol{q}+\boldsymbol{Q})} \delta_{\boldsymbol{k}_3+\boldsymbol{G}_3,\boldsymbol{k}_2+\boldsymbol{G}_2-(\boldsymbol{q}+\boldsymbol{Q})} \times \\
& \qquad V_{\alpha\alpha'}(\boldsymbol{q}+\boldsymbol{Q}) u^*_{\alpha,\boldsymbol{k}_4+\boldsymbol{G}_4;n_4} \hat{d}^\dagger_{\boldsymbol{k}_4;n_4} u^*_{\alpha',\boldsymbol{k}_3+\boldsymbol{G}_3;n_3} \hat{d}^\dagger_{\boldsymbol{k}_3;n_3} u_{\alpha',\boldsymbol{k}_2+\boldsymbol{G}_2;n_2} \hat{d}_{\boldsymbol{k}_2;n_2} u_{\alpha,\boldsymbol{k}_1+\boldsymbol{G}_1;n_1} \hat{d}_{\boldsymbol{k}_1;n_1} \\
=& \frac{1}{2N_s} \sum_{\boldsymbol{k}_{1-4},n_{1-4}} \hat{d}^\dagger_{\boldsymbol{k}_4;n_4} \hat{d}^\dagger_{\boldsymbol{k}_3;n_3} \hat{d}_{\boldsymbol{k}_2;n_2} \hat{d}_{\boldsymbol{k}_1;n_1} \sum_{\alpha\alpha',\boldsymbol{G}_{1-4}} \delta_{\boldsymbol{k}_4+\boldsymbol{G}_4,\boldsymbol{k}_1+\boldsymbol{G}_1+(\boldsymbol{q}+\boldsymbol{Q})} \delta_{\boldsymbol{k}_3+\boldsymbol{G}_3,\boldsymbol{k}_2+\boldsymbol{G}_2-(\boldsymbol{q}+\boldsymbol{Q})} \\
& \qquad V_{\alpha\alpha'}(\boldsymbol{q}+\boldsymbol{Q}) u^*_{\alpha,\boldsymbol{k}_4+\boldsymbol{G}_4;n_4} u^*_{\alpha',\boldsymbol{k}_3+\boldsymbol{G}_3;n_3} u_{\alpha',\boldsymbol{k}_2+\boldsymbol{G}_2;n_2} u_{\alpha,\boldsymbol{k}_1+\boldsymbol{G}_1;n_1} \\
=& \frac{1}{2N_s} \sum_{\boldsymbol{k}_{1-4},n_{1-4}} \hat{d}^\dagger_{\boldsymbol{k}_4;n_4} \hat{d}^\dagger_{\boldsymbol{k}_3;n_3} \hat{d}_{\boldsymbol{k}_2;n_2} \hat{d}_{\boldsymbol{k}_1;n_1} V_{n_4 n_3 n_2 n_1}(\boldsymbol{k}_1, \boldsymbol{k}_2, \boldsymbol{k}_3, \boldsymbol{k}_4)
\end{aligned} \tag{65}$$

where

$$\begin{aligned}
V_{n_4 n_3 n_2 n_1}(\boldsymbol{k}_1, \boldsymbol{k}_2, \boldsymbol{k}_3, \boldsymbol{k}_4) = & \sum_{\alpha\alpha',\boldsymbol{G}_{1-4}} \delta_{\boldsymbol{k}_4+\boldsymbol{G}_4,\boldsymbol{k}_1+\boldsymbol{G}_1+(\boldsymbol{q}+\boldsymbol{Q})} \delta_{\boldsymbol{k}_3+\boldsymbol{G}_3,\boldsymbol{k}_2+\boldsymbol{G}_2-(\boldsymbol{q}+\boldsymbol{Q})} \\
& V_{\alpha\alpha'}(\boldsymbol{q}+\boldsymbol{Q}) u^*_{\alpha,\boldsymbol{k}_4+\boldsymbol{G}_4;n_4} u^*_{\alpha',\boldsymbol{k}_3+\boldsymbol{G}_3;n_3} u_{\alpha',\boldsymbol{k}_2+\boldsymbol{G}_2;n_2} u_{\alpha,\boldsymbol{k}_1+\boldsymbol{G}_1;n_1}
\end{aligned} \tag{66}$$

In Hartee-Fock approximation, only items satisfying $\delta_{\boldsymbol{k}_1,\boldsymbol{k}_4}\delta_{\boldsymbol{k}_2,\boldsymbol{k}_3} = 1$ or $\delta_{\boldsymbol{k}_1,\boldsymbol{k}_3}\delta_{\boldsymbol{k}_2,\boldsymbol{k}_4} = 1$ do matter. For both of two cases, $\boldsymbol{G}_4 = \boldsymbol{G}_1 + \boldsymbol{Q}, \boldsymbol{G}_3 = \boldsymbol{G}_2 - \boldsymbol{Q}$. This leads to

$$\begin{aligned}
V_{n_4 n_3 n_2 n_1}(\boldsymbol{k}_1, \boldsymbol{k}_2, \boldsymbol{k}_3, \boldsymbol{k}_4) = & \sum_{\alpha\alpha',\boldsymbol{G}_{1-4},\boldsymbol{Q}} \delta_{\boldsymbol{k}_4,\boldsymbol{k}_1+\boldsymbol{q}} \delta_{\boldsymbol{k}_3,\boldsymbol{k}_2-\boldsymbol{q}} \delta_{\boldsymbol{G}_4,\boldsymbol{G}_1+\boldsymbol{Q}} \delta_{\boldsymbol{G}_3,\boldsymbol{G}_2-\boldsymbol{Q}} \\
& V_{\alpha\alpha'}(\boldsymbol{q}+\boldsymbol{Q}) u^*_{\alpha,\boldsymbol{k}_4+\boldsymbol{G}_4;n_4} u^*_{\alpha',\boldsymbol{k}_3+\boldsymbol{G}_3;n_3} u_{\alpha',\boldsymbol{k}_2+\boldsymbol{G}_2;n_2} u_{\alpha,\boldsymbol{k}_1+\boldsymbol{G}_1;n_1} \\
= & \sum_{\alpha\alpha',\boldsymbol{Q}} \delta_{\boldsymbol{k}_4,\boldsymbol{k}_1+\boldsymbol{q}} \delta_{\boldsymbol{k}_3,\boldsymbol{k}_2-\boldsymbol{q}} V_{\alpha\alpha'}(\boldsymbol{q}+\boldsymbol{Q}) \\
& \left(\sum_{\boldsymbol{G}_1,\boldsymbol{G}_4} \delta_{\boldsymbol{G}_4,\boldsymbol{G}_1+\boldsymbol{Q}} u^*_{\alpha,\boldsymbol{k}_4+\boldsymbol{G}_4;n_4} u_{\alpha,\boldsymbol{k}_1+\boldsymbol{G}_1;n_1} \right) \left(\sum_{\boldsymbol{G}_2,\boldsymbol{G}_3} \delta_{\boldsymbol{G}_3,\boldsymbol{G}_2-\boldsymbol{Q}} u^*_{\alpha',\boldsymbol{k}_3+\boldsymbol{G}_3;n_3} u_{\alpha',\boldsymbol{k}_2+\boldsymbol{G}_2;n_2} \right) \\
= & \sum_{\alpha\alpha',\boldsymbol{Q}} \delta_{\boldsymbol{k}_4,\boldsymbol{k}_1+\boldsymbol{q}} \delta_{\boldsymbol{k}_3,\boldsymbol{k}_2-\boldsymbol{q}} V_{\alpha\alpha'}(\boldsymbol{q}+\boldsymbol{Q}) \Lambda^{\alpha}_{\boldsymbol{Q},\boldsymbol{k}_4,\boldsymbol{k}_1;n_4,n_1} \Lambda^{\alpha'}_{-\boldsymbol{Q},\boldsymbol{k}_3,\boldsymbol{k}_2;n_3,n_2}
\end{aligned} \tag{67}$$

where

$$\begin{aligned}
\Lambda^{\alpha}_{\boldsymbol{Q},\boldsymbol{k}_4,\boldsymbol{k}_1;n_4,n_1} &= \sum_{\boldsymbol{G}_1,\boldsymbol{G}_4} \delta_{\boldsymbol{G}_4,\boldsymbol{G}_1+\boldsymbol{Q}} u^*_{\alpha,\boldsymbol{k}_4+\boldsymbol{G}_4;n_4} u_{\alpha,\boldsymbol{k}_1+\boldsymbol{G}_1;n_1} \\
\Lambda^{\alpha'}_{-\boldsymbol{Q},\boldsymbol{k}_3,\boldsymbol{k}_2;n_3,n_2} &= \sum_{\boldsymbol{G}_2,\boldsymbol{G}_3} \delta_{\boldsymbol{G}_3,\boldsymbol{G}_2-\boldsymbol{Q}} u^*_{\alpha',\boldsymbol{k}_3+\boldsymbol{G}_3;n_3} u_{\alpha',\boldsymbol{k}_2+\boldsymbol{G}_2;n_2}
\end{aligned} \tag{68}$$

In calculation, if $V(\boldsymbol{q})$ does not relay on α, we denote

$$V_{n_4n_3n_2n_1}(\boldsymbol{k}_1,\boldsymbol{k}_2,\boldsymbol{k}_3,\boldsymbol{k}_4)=\sum_{\boldsymbol{Q}}\delta_{\boldsymbol{k}_4,\boldsymbol{k}_1+\boldsymbol{q}}\delta_{\boldsymbol{k}_3,\boldsymbol{k}_2-\boldsymbol{q}}V(\boldsymbol{q}+\boldsymbol{Q})\Lambda_{\boldsymbol{Q},\boldsymbol{k}_4,\boldsymbol{k}_1;n_4,n_1}\Lambda_{-\boldsymbol{Q},\boldsymbol{k}_3,\boldsymbol{k}_2;n_3,n_2} \tag{69}$$

where

$$\begin{aligned}\Lambda_{\boldsymbol{Q},\boldsymbol{k}_4,\boldsymbol{k}_1;n_4,n_1}&=\sum_{\boldsymbol{G}_1,\boldsymbol{G}_4,\alpha}\delta_{\boldsymbol{G}_4,\boldsymbol{G}_1+\boldsymbol{Q}}u^*_{\alpha,\boldsymbol{k}_4+\boldsymbol{G}_4;n_4}u_{\alpha,\boldsymbol{k}_1+\boldsymbol{G}_1;n_1}\\ \Lambda_{-\boldsymbol{Q},\boldsymbol{k}_3,\boldsymbol{k}_2;n_3,n_2}&=\sum_{\boldsymbol{G}_2,\boldsymbol{G}_3,\alpha'}\delta_{\boldsymbol{G}_3,\boldsymbol{G}_2-\boldsymbol{Q}}u^*_{\alpha',\boldsymbol{k}_3+\boldsymbol{G}_3;n_3}u_{\alpha',\boldsymbol{k}_2+\boldsymbol{G}_2;n_2}\end{aligned} \tag{70}$$

satisfying

$$\Lambda_{\boldsymbol{Q},\boldsymbol{k}_2,\boldsymbol{k}_1;n_2,n_1}=\sum_{\boldsymbol{G}_1,\boldsymbol{G}_2}\delta_{\boldsymbol{G}_2,\boldsymbol{G}_1+\boldsymbol{Q}}\sum_{\alpha}u^*_{\alpha,\boldsymbol{k}_2+\boldsymbol{G}_2;n_2}u_{\alpha,\boldsymbol{k}_1+\boldsymbol{G}_1;n_1} \tag{71}$$

l,l' layer, α,α' sublattice in multilayer graphene/tMoTe2.

Next we denote the single-particle density matrix as $\rho_{n_2,n_1}(\boldsymbol{k})=\hat{d}^\dagger_{\boldsymbol{k};n_2}\hat{d}_{\boldsymbol{k};n_1}$. We assume that the system is homogeneous: $\langle\hat{d}^\dagger_{\boldsymbol{k}_2;n_2}\hat{d}_{\boldsymbol{k}_1;n_1}\rangle=\langle\hat{d}^\dagger_{\boldsymbol{k}_2;n_2}\hat{d}_{\boldsymbol{k}_1;n_1}\rangle\delta_{\boldsymbol{k}_2,\boldsymbol{k}_1}=\rho_{n_2,n_1}(\boldsymbol{k}_1)\delta_{\boldsymbol{k}_2,\boldsymbol{k}_1}$.

Recalling the Hartee-Fock approximation

$$\hat{A}\hat{B}\approx<\hat{A}>\hat{B}+\hat{A}<\hat{B}>-<\hat{A}><\hat{B}>, \tag{72}$$

we get

$$\begin{aligned}\hat{H}^{\mathrm{H}}=&\frac{1}{2N_s}\sum_{\boldsymbol{k}_{1-4}}\sum_{n_1n_2n_3n_4}V_{n_4n_3n_2n_1}(\boldsymbol{k}_1,\boldsymbol{k}_2,\boldsymbol{k}_3,\boldsymbol{k}_4)\hat{d}^\dagger_{\boldsymbol{k}_4;n_4}\hat{d}^\dagger_{\boldsymbol{k}_3;n_3}\hat{d}_{\boldsymbol{k}_2;n_2}\hat{d}_{\boldsymbol{k}_1;n_1}\\
=&\frac{1}{2N_s}\sum_{\boldsymbol{k}_{1-4}}\sum_{n_1n_2n_3n_4}V_{n_4n_3n_2n_1}(\boldsymbol{k}_1,\boldsymbol{k}_2,\boldsymbol{k}_3,\boldsymbol{k}_4)\hat{d}^\dagger_{\boldsymbol{k}_3;n_3}\hat{d}_{\boldsymbol{k}_2;n_2}\hat{d}^\dagger_{\boldsymbol{k}_4;n_4}\hat{d}_{\boldsymbol{k}_1;n_1}\\
\approx&\frac{1}{2N_s}\sum_{\boldsymbol{k}_{1-4}}\sum_{n_1n_2n_3n_4}V_{n_4n_3n_2n_1}(\boldsymbol{k}_1,\boldsymbol{k}_2,\boldsymbol{k}_3,\boldsymbol{k}_4)\\
&\left[\langle\hat{d}^\dagger_{\boldsymbol{k}_3;n_3}\hat{d}_{\boldsymbol{k}_2;n_2}\rangle\hat{d}^\dagger_{\boldsymbol{k}_4;n_4}\hat{d}_{\boldsymbol{k}_1;n_1}+\hat{d}^\dagger_{\boldsymbol{k}_3;n_3}\hat{d}_{\boldsymbol{k}_2;n_2}\langle\hat{d}^\dagger_{\boldsymbol{k}_4;n_4}\hat{d}_{\boldsymbol{k}_1;n_1}\rangle-\langle\hat{d}^\dagger_{\boldsymbol{k}_3;n_3}\hat{d}_{\boldsymbol{k}_2;n_2}\rangle\langle\hat{d}^\dagger_{\boldsymbol{k}_4;n_4}\hat{d}_{\boldsymbol{k}_1;n_1}\rangle\right]\\
=&\frac{1}{2N_s}\sum_{\boldsymbol{k}_{1-4}}\sum_{n_1n_2n_3n_4}V_{n_4n_3n_2n_1}(\boldsymbol{k}_1,\boldsymbol{k}_2,\boldsymbol{k}_3,\boldsymbol{k}_4)\\
&\left[\rho_{n_3,n_2}(\boldsymbol{k}_2)\delta_{\boldsymbol{k}_2,\boldsymbol{k}_3}\hat{d}^\dagger_{\boldsymbol{k}_4;n_4}\hat{d}_{\boldsymbol{k}_1;n_1}+\hat{d}^\dagger_{\boldsymbol{k}_3;n_3}\hat{d}_{\boldsymbol{k}_2;n_2}\rho_{n_4,n_1}(\boldsymbol{k}_1)\delta_{\boldsymbol{k}_1,\boldsymbol{k}_4}-\rho_{n_3,n_2}(\boldsymbol{k}_2)\delta_{\boldsymbol{k}_2,\boldsymbol{k}_3}\rho_{n_4,n_1}(\boldsymbol{k}_1)\delta_{\boldsymbol{k}_1,\boldsymbol{k}_4}\right]\\
&\delta_{\boldsymbol{k}_2,\boldsymbol{k}_3},\delta_{\boldsymbol{k}_3+\boldsymbol{G}_3,\boldsymbol{k}_2+\boldsymbol{G}_2-(\boldsymbol{q}+\boldsymbol{Q})},\delta_{\boldsymbol{k}_4+\boldsymbol{G}_4,\boldsymbol{k}_1+\boldsymbol{G}_1+(\boldsymbol{q}+\boldsymbol{Q})}\Rightarrow\delta_{\boldsymbol{q},0},\delta_{\boldsymbol{k}_1,\boldsymbol{k}_4}\\
=&\frac{1}{2N_s}\sum_{\boldsymbol{k}_1\boldsymbol{k}_2}\sum_{n_1n_2n_3n_4}V_{n_4n_3n_2n_1}(\boldsymbol{k}_1,\boldsymbol{k}_2,\boldsymbol{k}_3=\boldsymbol{k}_2,\boldsymbol{k}_4=\boldsymbol{k}_1)\\
&\left[\rho_{n_3,n_2}(\boldsymbol{k}_2)\hat{d}^\dagger_{\boldsymbol{k}_1;n_4}\hat{d}_{\boldsymbol{k}_1;n_1}+\hat{d}^\dagger_{\boldsymbol{k}_2;n_3}\hat{d}_{\boldsymbol{k}_2;n_2}\rho_{n_4,n_1}(\boldsymbol{k}_1)-\rho_{n_3,n_2}(\boldsymbol{k}_2)\rho_{n_4,n_1}(\boldsymbol{k}_1)\right]\end{aligned} \tag{73}$$

$$
\begin{aligned}
\hat{H}^{\mathrm{F}} =& \frac{1}{2N_s}\sum_{\boldsymbol{k}_{1-4}}\sum_{n_1n_2n_3n_4} V_{n_4n_3n_2n_1}(\boldsymbol{k}_1,\boldsymbol{k}_2,\boldsymbol{k}_3,\boldsymbol{k}_4)\hat{d}^\dagger_{\boldsymbol{k}_4;n_4}\hat{d}^\dagger_{\boldsymbol{k}_3;n_3}\hat{d}_{\boldsymbol{k}_2;n_2}\hat{d}_{\boldsymbol{k}_1;n_1}\\
=& -\frac{1}{2N_s}\sum_{\boldsymbol{k}_{1-4}}\sum_{n_1n_2n_3n_4} V_{n_4n_3n_2n_1}(\boldsymbol{k}_1,\boldsymbol{k}_2,\boldsymbol{k}_3,\boldsymbol{k}_4)\hat{d}^\dagger_{\boldsymbol{k}_4;n_4}\hat{d}_{\boldsymbol{k}_2;n_2}\hat{d}^\dagger_{\boldsymbol{k}_3;n_3}\hat{d}_{\boldsymbol{k}_1;n_1}\\
\approx& -\frac{1}{2N_s}\sum_{\boldsymbol{k}_{1-4}}\sum_{n_1n_2n_3n_4} V_{n_4n_3n_2n_1}(\boldsymbol{k}_1,\boldsymbol{k}_2,\boldsymbol{k}_3,\boldsymbol{k}_4)\\
&\left[\langle\hat{d}^\dagger_{\boldsymbol{k}_4;n_4}\hat{d}_{\boldsymbol{k}_2;n_2}\rangle\hat{d}^\dagger_{\boldsymbol{k}_3;n_3}\hat{d}_{\boldsymbol{k}_1;n_1}+\hat{d}^\dagger_{\boldsymbol{k}_4;n_4}\hat{d}_{\boldsymbol{k}_2;n_2}\langle\hat{d}^\dagger_{\boldsymbol{k}_3;n_3}\hat{d}_{\boldsymbol{k}_1;n_1}\rangle-\langle\hat{d}^\dagger_{\boldsymbol{k}_4;n_4}\hat{d}_{\boldsymbol{k}_2;n_2}\rangle\langle\hat{d}^\dagger_{\boldsymbol{k}_3;n_3}\hat{d}_{\boldsymbol{k}_1;n_1}\rangle\right]\\
=& -\frac{1}{2N_s}\sum_{\boldsymbol{k}_{1-4}}\sum_{n_1n_2n_3n_4} V_{n_4n_3n_2n_1}(\boldsymbol{k}_1,\boldsymbol{k}_2,\boldsymbol{k}_3,\boldsymbol{k}_4)\\
&\left[\rho_{n_4,n_2}(\boldsymbol{k}_2)\delta_{\boldsymbol{k}_4,\boldsymbol{k}_2}\hat{d}^\dagger_{\boldsymbol{k}_3;n_3}\hat{d}_{\boldsymbol{k}_1;n_1}+\hat{d}^\dagger_{\boldsymbol{k}_4;n_4}\hat{d}_{\boldsymbol{k}_2;n_2}\rho_{n_3,n_1}(\boldsymbol{k}_1)\delta_{\boldsymbol{k}_3,\boldsymbol{k}_1}-\rho_{n_4,n_2}(\boldsymbol{k}_2)\delta_{\boldsymbol{k}_4,\boldsymbol{k}_2}\rho_{n_3,n_1}(\boldsymbol{k}_1)\delta_{\boldsymbol{k}_3,\boldsymbol{k}_1}\right]\\
&\delta_{\boldsymbol{k}_4,\boldsymbol{k}_2},\delta_{\boldsymbol{k}_3+\boldsymbol{G}_3,\boldsymbol{k}_2+\boldsymbol{G}_2-(\boldsymbol{q}+\boldsymbol{Q})},\delta_{\boldsymbol{k}_4+\boldsymbol{G}_4,\boldsymbol{k}_1+\boldsymbol{G}_1+(\boldsymbol{q}+\boldsymbol{Q})}\Rightarrow\delta_{\boldsymbol{k}_1,\boldsymbol{k}_3}\\
=& -\frac{1}{2N_s}\sum_{\boldsymbol{k}_1\boldsymbol{k}_2}\sum_{n_1n_2n_3n_4} V_{n_4n_3n_2n_1}(\boldsymbol{k}_1,\boldsymbol{k}_2,\boldsymbol{k}_3=\boldsymbol{k}_1,\boldsymbol{k}_4=\boldsymbol{k}_2)\\
&\left[\rho_{n_4,n_2}(\boldsymbol{k}_2)\hat{d}^\dagger_{\boldsymbol{k}_1;n_3}\hat{d}_{\boldsymbol{k}_1;n_1}+\hat{d}^\dagger_{\boldsymbol{k}_2;n_4}\hat{d}_{\boldsymbol{k}_2;n_2}\rho_{n_3,n_1}(\boldsymbol{k}_1)-\rho_{n_4,n_2}(\boldsymbol{k}_2)\rho_{n_3,n_1}(\boldsymbol{k}_1)\right]
\end{aligned}
\tag{74}
$$

Note for either $\boldsymbol{k}_2=\boldsymbol{k}_3,\boldsymbol{k}_1=\boldsymbol{k}_4$, or $\boldsymbol{k}_1=\boldsymbol{k}_3,\boldsymbol{k}_2=\boldsymbol{k}_4$, one have $\boldsymbol{G}_1+\boldsymbol{G}_2=\boldsymbol{G}_3+\boldsymbol{G}_4$.

The mean-field Hamiltonian becomes:

$$\hat{H}^{\mathrm{MF}} = h_0 + h_{\mathrm{HF}} - E_c \tag{75}$$

where

$$h_0 = \sum_{\boldsymbol{k}}\sum_{n}\epsilon_n(\boldsymbol{k})\hat{d}^\dagger_{\boldsymbol{k};n}\hat{d}_{\boldsymbol{k};n} \tag{76}$$

$$
\begin{aligned}
h_{\mathrm{HF}} =& \frac{1}{2N_s}\sum_{\boldsymbol{k}_1\boldsymbol{k}_2}\sum_{n_1n_2n_3n_4}\{\\
&V_{n_4n_3n_2n_1}(\boldsymbol{k}_1,\boldsymbol{k}_2,\boldsymbol{k}_3=\boldsymbol{k}_2,\boldsymbol{k}_4=\boldsymbol{k}_1)\left[\rho_{n_3,n_2}(\boldsymbol{k}_2)\left[\hat{d}^\dagger\hat{d}\right]_{n_4,n_1}(\boldsymbol{k}_1)+\rho_{n_4,n_1}(\boldsymbol{k}_1)\hat{d}^\dagger_{\boldsymbol{k}_2;n_3}\hat{d}_{\boldsymbol{k}_2;n_2}\right]\\
&-V_{n_4n_3n_2n_1}(\boldsymbol{k}_1,\boldsymbol{k}_2,\boldsymbol{k}_3=\boldsymbol{k}_1,\boldsymbol{k}_4=\boldsymbol{k}_2)\left[\rho_{n_4,n_2}(\boldsymbol{k}_2)\hat{d}^\dagger_{\boldsymbol{k}_1;n_3}\hat{d}_{\boldsymbol{k}_1;n_1}+\hat{d}^\dagger_{\boldsymbol{k}_2;n_4}\hat{d}_{\boldsymbol{k}_2;n_2}\rho_{n_3,n_1}(\boldsymbol{k}_1)\right]\}
\end{aligned}
\tag{77}
$$

and

$$
\begin{aligned}
E_c = \frac{1}{2N_s}\sum_{\boldsymbol{k}_1\boldsymbol{k}_2}\sum_{n_1n_2n_3n_4}\{\quad & V_{n_4n_3n_2n_1}(\boldsymbol{k}_1,\boldsymbol{k}_2,\boldsymbol{k}_3=\boldsymbol{k}_2,\boldsymbol{k}_4=\boldsymbol{k}_1)\rho_{n_3,n_2}(\boldsymbol{k}_2)\rho_{n_4,n_1}(\boldsymbol{k}_1)\\
& -V_{n_4n_3n_2n_1}(\boldsymbol{k}_1,\boldsymbol{k}_2,\boldsymbol{k}_3=\boldsymbol{k}_1,\boldsymbol{k}_4=\boldsymbol{k}_2)\rho_{n_4,n_2}(\boldsymbol{k}_2)\rho_{n_3,n_1}(\boldsymbol{k}_1)\}
\end{aligned}
\tag{78}
$$

Next let us simplify the problem. 1) In two-body interaction, let us set $n_1 = n_4 = n, n_2 = n_3 = m$ for the inter-band interaction:

$$\hat{H}^{\text{int}} = \frac{1}{2N_s} \sum_{\boldsymbol{k}_{1-4},n,m} \hat{d}^{\dagger}_{\boldsymbol{k}_4;n} \hat{d}^{\dagger}_{\boldsymbol{k}_3;m} \hat{d}_{\boldsymbol{k}_2;m} \hat{d}_{\boldsymbol{k}_1;n} V_{nmmn}(\boldsymbol{k}_1, \boldsymbol{k}_2, \boldsymbol{k}_3, \boldsymbol{k}_4) \tag{79}$$

The mean-field Hamiltonian becomes:

$$\hat{H}^{\text{MF}} = h_0 + h_{\text{HF}} - E_c \tag{80}$$

where

$$h_0 = \sum_{\boldsymbol{k}} \sum_{n} \epsilon_n(\boldsymbol{k}) \hat{d}^{\dagger}_{\boldsymbol{k};n} \hat{d}_{\boldsymbol{k};n} \tag{81}$$

$$\begin{aligned} h_{\text{HF}} = \frac{1}{2N_s} \sum_{\boldsymbol{k}_1\boldsymbol{k}_2} \sum_{nm} \{ & V_{nmmn}(\boldsymbol{k}_1, \boldsymbol{k}_2, \boldsymbol{k}_3 = \boldsymbol{k}_2, \boldsymbol{k}_4 = \boldsymbol{k}_1) \left[\rho_{m,m}(\boldsymbol{k}_2) \hat{d}^{\dagger}_{\boldsymbol{k}_1,n} \hat{d}_{\boldsymbol{k}_1,n} + \rho_{n,n}(\boldsymbol{k}_1) \hat{d}^{\dagger}_{\boldsymbol{k}_2;m} \hat{d}_{\boldsymbol{k}_2;m} \right] \\ & - V_{nmmn}(\boldsymbol{k}_1, \boldsymbol{k}_2, \boldsymbol{k}_3 = \boldsymbol{k}_1, \boldsymbol{k}_4 = \boldsymbol{k}_2) \left[\rho_{n,m}(\boldsymbol{k}_2) \hat{d}^{\dagger}_{\boldsymbol{k}_1;m} \hat{d}_{\boldsymbol{k}_1;n} + \hat{d}^{\dagger}_{\boldsymbol{k}_2;n} \hat{d}_{\boldsymbol{k}_2;m} \rho_{m,n}(\boldsymbol{k}_1) \right] \} \end{aligned} \tag{82}$$

and

$$E_c = \frac{1}{2N_s} \sum_{\boldsymbol{k}_1\boldsymbol{k}_2} \sum_{nmmn} \{ \quad V_{nmmn}(\boldsymbol{k}_1, \boldsymbol{k}_2, \boldsymbol{k}_3 = \boldsymbol{k}_2, \boldsymbol{k}_4 = \boldsymbol{k}_1) \rho_{m,m}(\boldsymbol{k}_2) \rho_{n,n}(\boldsymbol{k}_1) \tag{83}$$

$$- V_{nmmn}(\boldsymbol{k}_1, \boldsymbol{k}_2, \boldsymbol{k}_3 = \boldsymbol{k}_1, \boldsymbol{k}_4 = \boldsymbol{k}_2) \rho_{n,m}(\boldsymbol{k}_2) \rho_{m,n}(\boldsymbol{k}_1) \} \tag{84}$$

2) In two-body interaction, let us set $n_1 = n_3 = n, n_2 = n_4 = m$ for the inter-band interaction:

$$\hat{H}^{\text{int}} = \frac{1}{2N_s} \sum_{\boldsymbol{k}_{1-4},n,m} \hat{d}^{\dagger}_{\boldsymbol{k}_4;m} \hat{d}^{\dagger}_{\boldsymbol{k}_3;n} \hat{d}_{\boldsymbol{k}_2;m} \hat{d}_{\boldsymbol{k}_1;n} V_{mnmn}(\boldsymbol{k}_1, \boldsymbol{k}_2, \boldsymbol{k}_3, \boldsymbol{k}_4) \tag{85}$$

The mean-field Hamiltonian becomes:

$$\hat{H}^{\text{MF}} = h_0 + h_{\text{HF}} - E_c \tag{86}$$

where

$$\begin{aligned} h_{\text{HF}} = \frac{1}{2N_s} \sum_{\boldsymbol{k}_1\boldsymbol{k}_2} \sum_{nm} \{ & V_{mnmn}(\boldsymbol{k}_1, \boldsymbol{k}_2, \boldsymbol{k}_3 = \boldsymbol{k}_2, \boldsymbol{k}_4 = \boldsymbol{k}_1) \left[\rho_{n,m}(\boldsymbol{k}_2) \hat{d}^{\dagger}_{\boldsymbol{k}_1,m} \hat{d}_{\boldsymbol{k}_1,n} + \rho_{m,n}(\boldsymbol{k}_1) \hat{d}^{\dagger}_{\boldsymbol{k}_2;n} \hat{d}_{\boldsymbol{k}_2;m} \right] \\ & - V_{mnmn}(\boldsymbol{k}_1, \boldsymbol{k}_2, \boldsymbol{k}_3 = \boldsymbol{k}_1, \boldsymbol{k}_4 = \boldsymbol{k}_2) \left[\rho_{m,m}(\boldsymbol{k}_2) \hat{d}^{\dagger}_{\boldsymbol{k}_1;n} \hat{d}_{\boldsymbol{k}_1;n} + \hat{d}^{\dagger}_{\boldsymbol{k}_2;m} \hat{d}_{\boldsymbol{k}_2;m} \rho_{n,n}(\boldsymbol{k}_1) \right] \} \end{aligned} \tag{87}$$

and

$$E_c = \frac{1}{2N_s} \sum_{\boldsymbol{k}_1\boldsymbol{k}_2} \sum_{nmmn} \{ \quad V_{mnmn}(\boldsymbol{k}_1, \boldsymbol{k}_2, \boldsymbol{k}_3 = \boldsymbol{k}_2, \boldsymbol{k}_4 = \boldsymbol{k}_1) \rho_{m,n}(\boldsymbol{k}_2) \rho_{n,m}(\boldsymbol{k}_1) \tag{88}$$

$$- V_{mnmn}(\boldsymbol{k}_1, \boldsymbol{k}_2, \boldsymbol{k}_3 = \boldsymbol{k}_1, \boldsymbol{k}_4 = \boldsymbol{k}_2) \rho_{m,m}(\boldsymbol{k}_2) \rho_{n,n}(\boldsymbol{k}_1) \} \tag{89}$$

HOMEWORK

1. Let us introduce the pair correlation function $g(r_2, r_1)$ which is defined as the normalized probability of finding an electron at position r_1 given that, at the same time, there is another electron at position r_2, i.e.

$$g(r_2, r_1) = \frac{1}{n(r_1)n(r_2)} \langle \sum_{i \neq j} \delta(r_1 - r_i)\delta(r_2 - r_j) \rangle \tag{90}$$

where the angular brackets denote here the average in the ground-state. Please calculate the pair function for weakly-interacting electrons in the framework of Hartee-Fock approximation. The noninteracting pair correlation This calculation will help you understand the picture of "exchange hole".

[1] V. Fock, Z. Phys. 61, 126–148 (1930); Z. Phys. 61, 795–805 (1930).

[2] S. Raghu, Xiao-Liang Qi, C. Honerkamp, Shou-Cheng Zhang, Phys.Rev.Lett. 100, 156401 (2008).

[3] Yann Claveau, Brice Arnaud, Sergio Di Matteo, arXiv.1403.2259

[4] Junkai Dong, Taige Wang, Tianle Wang, Tomohiro Soejima, Michael P. Zaletel, Ashvin Vishwanath, and Daniel E. Parker, Phys. Rev. Lett. 133, 206503 (2024); Zhihuan Dong, Adarsh S. Patri, and T. Senthil Phys. Rev. Lett. 133, 206502 (2024); Boran Zhou, Hui Yang, and Ya-Hui Zhang, Phys. Rev. Lett. 133, 206504 (2024); Tomohiro Soejima, Junkai Dong, Taige Wang, Tianle Wang, Michael P. Zaletel, Ashvin Vishwanath, and Daniel E. Parker, Phys. Rev. B 110, 205124 (2024)